METABOLIC SCALING
FROM INDIVIDUALS TO SOCIETIES

BY

MELANIE ELIZABETH MOSES

B.S., Symbolic Systems, Stanford University, 1993

DISSERTATION

Submitted in Partial Fulfillment of the
Requirements for the Degree of

Doctor of Philosophy
Biology

The University of New Mexico
Albuquerque, New Mexico

July, 2005

DEDICATION

For Inez Mason Henson, Rosa de la Vega and
Alejandro Mason Moses de la Vega

ACKNOWLEDGEMENTS

I would never have started, and certainly not completed, this dissertation without the love, encouragement and support of wonderful family, friends and colleagues.

My wife, Rosa de la Vega, has loved me enough to put up with tired and grumpy moods, encouraged me with pep talks and praise, supported me with big things like moving to the desert and little things like making me dinner, and a million things in between. Her impeccable attention to detail improved this dissertation quite a bit. Our son, Alejandro Moses de la Vega, has been so well behaved and patient that I could actually complete this work. He brings me immense joy every single day.

My grandmother, Inez Mason Henson, taught me that learning is fun. My mother, April Moses, taught me that I could do whatever I set my mind to. She alerted me to *Godel, Escher, Bach* and *Guns, Germs, and Steel* at just the right times, and early on, she recognized the importance of binocues. My father, John Moses, taught me the importance of rates of change, that you've got to write big to think big, and many other lessons that have gotten me through graduate school and life.

Andrea Quijada & KC Quirk returned me to sanity every Friday night. Young Women United continuously reminded me that things other than biology matter. Mai Dang ensured that entertaining diversions were only a mouse click away. The Draw Group stayed so close for so long, from so far away.

The UNM Biology Department, especially the Milne & Brown labs, and particularly Drew Allen, Krista Anderson, Nina Baum, Ethan Decker, Drew Kerkhoff, Matt Luck, Etsuko Nonaka, Jennifer Parody, Carla Restrepo, Horacio Samaniego, Ford Ballantyne, Morgan Ernest, James Gillooly, Allen Hurlbert, and Ethan White provided five years of friendship, inspiration and distractions.

My committee members Drs. Bruce Milne, Jim Brown and Ric Charnov have been excellent mentors and friends, and have taught me everything I know about biology. I particularly thank Bruce for countless improvements to this dissertation. Dr. Mike Kaspari served as an external reader and taught me that studying ants can be fun.

This work was supported by NSF through their Biocomplexity grant and Alliance for Graduate Education and the Professoriate (AGEP) Program, by the EPA Science to Achieve Results (STAR) Program, by the Sevilleta Long Term Ecological Research Site, and by UNM's Graduate Research and Development Grants.

I thank you all.

METABOLIC SCALING
FROM INDIVIDUALS TO SOCIETIES

BY

MELANIE ELIZABETH MOSES

ABSTRACT OF DISSERTATION

Submitted in Partial Fulfillment of the
Requirements for the Degree of

Doctor of Philosophy
Biology

The University of New Mexico
Albuquerque, New Mexico

July, 2005

METABOLIC SCALING

FROM INDIVIDUALS TO SOCIETIES

By

MELANIE E. MOSES

B.S., Symbolic Systems, Stanford University, 1993

Ph.D., Biology, University of New Mexico, 2005

ABSTRACT

The flux of energy and materials constrains all organisms. Allometric relationships between rates of energy consumption and other biological rates are manifest at many levels of biological organization. Here I examine relationships between social organization, energy consumption and reproductive rates. First, I present a model relating fertility rates to per capita energy consumption rates in contemporary human nations. Fertility declines as per capita energy consumption increases with a scaling exponent of -1/3 as predicted by allometric theory. Second, I examine the tradeoffs that occur between life history characteristics as mammals allocate energy to reproduction. The analysis shows that although reproductive effort is independent of adult mass, larger mammals have lower reproductive rates because they spend more time providing energy to grow each offspring. Third, I present the Allometric Network Travel and Search (ANTS) model of optimal colony foraging behavior as a function of colony size. Field observations of three *Pogonomyrmex* species show that large and small colonies employ different foraging strategies, each designed to minimize foraging time such that foraging

times of individual ants are very similar across a 30-fold difference in colony size. As a result, metabolic intake rates of colonies scale isometrically with the number of foragers in the colony. Finally, I show that because they integrate all parts of an individual or society, metabolic networks have allometric scaling of delivery capacity with network size. This common scaling behavior may lead to common patterns in energy acquisition and allocation in individuals and societies.

Table of Contents

LIST OF FIGURES

LIST OF TABLES

1 INTRODUCTION: A BIOLOGICAL APPROACH TO STUDYING SOCIAL METABOLISM

1.1 BACKGROUND

It is easy to imagine a human society as a super-organism. Roads and railways are its arteries and veins that distribute energy and materials throughout its territory. Oil wells and power plants are its lungs and heart, acquiring and transforming the energy that sustains it. Humans are its neurons, connected by wireless transmissions and telephone lines to direct, monitor and regulate its activities.

Such metaphors are thought provoking, but to study societies with the scientific tools of biology requires more than analogies. Here I examine metabolic patterns in human societies, individual mammals and ant colonies, and I investigate whether they are generated by common processes.

Biologists study life at different levels of organization. Cells are organized into organisms which can be organized into populations, communities, ecosystems, and societies. Frequently biologists study the processes by which lower level entities are organized into higher-level units; for example, how cells are integrated to form a functioning organism. There may also be feedback from a higher level that affects its constituent parts (Allen & Starr 1982). For example, the size of an organism constrains the metabolic rate of its cells (West *et al.* 2002). Likewise, properties of a society apparently constrain and influence the ecology, behavior, and life history of its individuals.

Howard Odum (1971, 1973) suggests that energy flows in societies could be studied in the same way they are studied in organisms and ecosystems. Social scientists have also considered energy flow to be a fundamental attribute of societies (White 1949, Rosa *et al.* 1988, Tainter 1990). These ideas have recently gained traction as ecologists study the metabolism of cities (Decker *et al.* 2002), ecological footprints of cities and regions (Luck *et al.* 2001), and the sustainability and ecological impacts of human societies (Vitousek *et al.* 1986 and 1997, Wackernagel *et al.* 2002). These studies focus on the external effects that human society has on other species, ecosystems, and the biosphere. While these external effects are of great significance, here I am interested in how the energy consumption of a society affects the ecology of the individuals who constitute that society.

1.2 Definitions and Tools

Metabolism is the rate at which energy is exchanged between an organism and its environment, transformed within an organism, and allocated to maintenance, growth and reproduction (Brown *et al*. 2004). Likewise, we can understand social metabolism as the rate at which energy is exchanged between a society and its environment, transformed within that society and allocated to maintenance, growth and, in some cases, reproduction of the society. In industrial societies, metabolism consists of consumption of all forms of fossil fuels, nuclear power, and electricity. This consumption can be referred to as industrial metabolism (Anderberg 1998).

Whole-organism metabolic rate scales as mass to the 3/4 power (Peters 1983, West *et al.* 1999) and most other biological rates, such as heart rate, reproductive rate and cellular metabolic rate, scale as mass to the -1/4 power (Peters 1983; Calder 1984; West *et al.* 1999). Metabolic theory posits that these scaling laws result from energetically efficient, space filling, fractal-like resource distribution networks such as the circulatory system of mammals or the vascular system of plants (West *et al.* 1999, 2000). Biological rates are ultimately limited not by mass, per se, but by rates of energy and material turnover.

Life is constrained by these fundamental allometric relationships at many levels of biological organization, including the level of mitochondrial activity within cells (West *et al*. 2002), the fertility rates of mammals and growth rates of populations (Charnov 1993), the population density of mammals and trees (Damuth 1981, Enquist *et al*. 1998) and foraging success in landscapes (Milne *et al.* 1992, Milne 1997). Scaling exponents are predictable despite extraordinary differences among these systems in network size and architecture, suggesting that there are fundamental tradeoffs between biological rates and power consumption. I apply the tools and approaches from metabolic theory to understand the ecological consequences of social metabolism on the individuals that constitute those societies.

1.3 Approach

I examine how the metabolic networks of societies constrain the ecology and behavior of individuals in those societies. In chapter 2, I show that modern human birth rates decrease

as industrial metabolic rates increases. The scaling of birth rate with industrial metabolism has the same scaling exponent as the scaling of birth rate with individual metabolic rate in mammals. Both patterns are predictable from metabolic theory.

Chapter 2 raises two interesting questions that I explore in subsequent chapters. First, in Chapter 3, I investigate the energetic basis of birth rate scaling in mammals. Birth rates decline as mammal body size increases because larger mammals provision their offspring with more energy in order to grow them to a larger size. Providing larger amounts of energy for growth takes a longer time, and that time is described by metabolic theory. If this same process occurs in modern human societies, we would expect birth rates to decline when humans have high requirements for industrial metabolism, as they do in industrialized nations.

Second, in Chapter 4, I investigate metabolic scaling in ant colonies to determine whether metabolism in societies follows the scaling rules of individuals. I show that some aspects of ant foraging change as the size of the colony increases. In particular, the time and distance foragers spend traveling to acquire resources scales allometrically with the number of foragers in the colony.

In Chapter 5, I show that the geometric scaling that describes ant foraging distances has the same mathematical basis as metabolic scaling in mammals and other individual organisms, even though the ants are not necessarily using fractal branching networks to acquire energy. This suggests that social networks operating in three dimensions can generate 1/4 power scaling, even when the network geometry is very different from biological networks. This supports the hypothesis that the metabolic scaling of human birth rates is similar to the metabolic scaling of mammalian birth rates

because industrial metabolic networks operate with delivery efficiency that is similar to that of biological networks.

1.4 REFERENCES

Allen, T.F.H. & Starr, T.B. (1982). *Hierarchy: Perspectives for ecological complexity*. The University of Chicago Press, Chicago.

Anderberg, S. (1998). Industrial metabolism and the linkages between economics, ethics and the environment. *Ecol. Econ.,* **24**, 311-320.

Brown, J.H., Gillooly, J.F., Allen, A.P., Savage, V.M. & West, G.B. (2004). Toward a metabolic theory of ecology. *Ecology,* **85**, 1771-1789.

Calder, W.A. (1984). *Size, Function and Life History*. Harvard Univ. Press, Cambridge, MA.

Charnov, E.L. (1993). *Life History Invariants*. Oxford University Press, New York.

Damuth, J. (1981). Population density and body size in mammals. *Nature*, **290,** 699–700.

Decker, E.H., Elliott, S., Smith, F.A., Blacke, D.R. & Rowland, F. S. (2000). Energy and material flow through the urban ecosystem. *Annu. Rev. Energy and Env.,* **25**, 685-740.

Enquist, B.J., Brown, J.H. & West, G.B. (1998). Allometric scaling of plant energetics and population density. *Nature*, **395**, 163–165.

Luck, M.A., Jenerette, G.D., Wu, J. & Grimm, N.B. (2001). The Urban Funnel Model and the Spatially Heterogeneous Ecological Footprint. *Ecosystems,* **4**, 782–796.

Milne, B.T., Turner, M.G., Wiens, J.A. & Johnson, A.R. (1992). Interactions between the fractal geometry of landscapes and allometric herbivory. *Theor. Popul. Bio.,* **41**, 337-353.

Milne, B.T. (1997). Applications of fractal geometry in wildlife biology. In *Wildlife and Landscape Ecology: Effects of Pattern and Scale* (ed. Bissonette, J.). Springer, New York, 32-69.

Odum, H.T. (1971). *Environment, Power and Society*. Wiley, New York.

Odum, H.T. (1973). Energy, ecology and economics. *Ambio,* **6**, 220-227.

Peters, R.H. (1983). *The Ecological Implications of Body Size*. Cambridge University Press, Cambridge.

Rosa, E.A., Machlis, G.E. & Keating, K.M. (1988) Energy and society. *Annu. Rev. Sociol.*, **14**, 149-172.

Tainter, J. (1990). *The Collapse of Complex Societies*. Cambridge University Press, Cambridge.

Vitousek, P.M., Ehrlich, P.R., Ehrlich, A.H. & Matson, P.A. (1986). Human appropriation of the products of photosynthesis. *Bioscience*, **36**, 368–373.

Vitousek, P.M., Mooney, H.A., Lubchenco, J. & Melillo, J.M. (1997). Human domination of Earth's ecosystems. *Science*, **277**, 494–499.

Wackernagel, M., Schulz, N.B., Deumling, D., Linares, A.C., Jenkins, M., Kapos, V., Monfreda, C., Loh, J., Myers, N., Norgaard, R. & Randers, J. (2002). Tracking the ecological overshoot of the human economy. *Proc. Natl. Acad. Sci. USA*, **99**, 9266–9271.

West, G.B., Brown, J.H. & Enquist, B.J. (1999). The fourth dimension of life: Fractal geometry and allometric scaling of organisms. *Science*, **284**, 1677–1679.

West, G.B., Brown, J.H. & Enquist, B.J. (2000). Scaling in biology: Patterns and processes, causes and consequences. In *Scaling in Biology* (eds. Brown, J.H. & West, G.B.). Oxford University Press, Oxford, 87–112.

West, G.B., Woodruff, W.H. & Brown, J.H. (2002). Allometric scaling of metabolic rate from molecules and mitochondria to cells and mammals. *Proc. Natl. Acad. Sci. USA*, **99**, 2473–2478.

White, L. (1949). *Energy and the evolution of culture*. In *The Science of Culture*. Farrar, Straus, Giroux, New York, 363-393.

2 THE ALLOMETRY OF HUMAN FERTILITY AND ENERGY USE

2.1 ABSTRACT

The flux of energy and materials constrains all organisms. Allometric relationships between rates of energy consumption and other biological rates are manifest at many levels of biological organization. Although human ecology is unusual in many respects, human populations also face energetic constraints. Here we present a model relating fertility rates to per capita energy consumption rates in contemporary human nations. Fertility declines as energy consumption increases with a scaling exponent of -1/3 as predicted by allometric theory. The decline may be explained by parental trade-offs between the number of children and the energetic investment in each child. We hypothesize that the -1/3 exponent results from the scaling properties of the networked infrastructure that delivers energy to consumers. This allometric analysis of human fertility offers a framework for understanding the demographic transition to smaller family sizes, with implications for human population growth, resource use and sustainability. This chapter was coauthored by James H. Brown (Department of Biology, University of New Mexico). It was published in *Ecology Letters*, Volume 6, 2003, pp. 295-300.

2.2 INTRODUCTION

Relationships between body size, metabolism, and biological rates and times result from fundamental allometric constraints on the structure and function of individual organisms (Peters 1983, West *et al.* 2000). Recent theory proposes that these ubiquitous empirical patterns occur because organisms have been selected to simultaneously maximize metabolic capacity and the efficiency of internal energy transport (West *et al.* 1999).

Modern humans are unique in that energy consumption is not limited by body mass and metabolic rate, but by the ability to harness non-metabolic energy such as gas, oil, coal, and nuclear, solar and hydroelectric power. Here we examine how modern human fertility varies with per capita energy consumption. Interestingly, modern fertility rates are largely a matter of choice, and like energy consumption, are not solely determined by human physiology. Still, human fertility varies with energy consumption in accordance with allometric predictions. This raises the possibilities that allometry may describe non-biological energy distribution networks and that human reproductive choices may ultimately be guided by that allometry.

Allometric scaling relationships are described by power functions that relate dependent variables to body mass. Whole-organism metabolic rate, or the rate of energy consumption, scales as mass to the 3/4 power (Peters 1983, West *et al.* 1999):

$$B = B_0 M^{3/4} \qquad [2.1]$$

where B is the metabolic rate, M is body mass and B_0 is a scaling constant. Most other biological rates (R), such as heart rate, reproductive rate or cellular metabolic rate, are

predicted and observed to scale as mass to the -1/4 power (Peters 1983; West *et al.* 1999, 2000):

$$R \sim M^{-1/4} \qquad [2.2]$$

These scaling laws follow from allometric theory in which metabolism is limited by an energetically efficient, space filling, fractal-like resource distribution network, such as the circulatory system of mammals or the vascular system of plants (West *et al.* 1999, 2000). Biological rates are ultimately limited not by mass, per se, but by rates of energy and material turnover. Re-arranging the relationships in 2.1 and 2.2 shows the predicted relationship between metabolic rate and other biological rates:

$$R \sim B^{-1/3} \qquad [2.3]$$

Life is constrained by these fundamental allometric relationships at many levels of biological organization, including the level of mitochondrial activity within cells (West *et al*. 2002), the fertility rates of mammals and growth rates of populations (Charnov 1993), and the population density of mammals and trees (Damuth 1981, Enquist *et al*. 1998). Scaling exponents are predictable despite extraordinary differences among these systems in network size and architecture, suggesting that there are fundamental tradeoffs between biological rates and power consumption. We suggest that these trade-offs constrain human fertility as well.

Although humans are highly unusual organisms in many respects, most characteristics of human physiology are predictable from scaling relationships observed in other mammals, particularly primates. For example, human metabolic rate can be predicted by allometric equations. By using the empirically determined $B_0 = 5.66$ for higher primates (Peters 1983), Equation 2.1 predicts that the metabolic rate of a 60-kilogram human is 120 watts or 2500 calories per day. However, humans differ from other organisms in their social organization and ecology. The exploitation of supplemental energy sources has fueled 10,000 years of exponential human population growth (Cipolla 1972), the development of modern industrial–technological societies, and the rise of *Homo sapiens* to become the dominant species on earth, with major impacts on global biodiversity, biogeochemical cycles and climate (Vitousek *et al.* 1986, 1997).

Biological metabolism is a small fraction of the total energy consumed by modern humans who utilize vast distribution networks to extract and deliver oil, gas, coal, electricity and other resources. These energy resources constitute the metabolism of modern industrial societies. Per capita consumption of this industrial metabolism varies from a few hundred watts in the poorest nations, to many thousands of watts in more industrial countries, which rely predominantly on fossil fuels (World Resources Institute 2000). The per capita rate of industrial metabolism in the United States is 11,000 W (World Resources Institute 2000) which is approximately 100 times the rate of biological metabolism and, from Equation 2.1, is the estimated rate of energy consumption of a 30,000-kg primate.

2.3 METHODS

We used data from over 100 nations from 1970 to 1997 (World Resources Institute 2000) to test the hypothesis that industrial metabolism and birth rates are related by Relation 2.3. Demographic data consist of total fertility rates (projected lifetime births per woman based on age-specific annual fertility), crude fertility rates (births per 1000 population per year) and infant mortality rates (deaths per 1000 live births) for each nation. Per capita industrial metabolism is the per capita share of the total energy consumed by each nation. These values were converted into watts and averaged to correspond with 5-year averages of demographic data. Additional data covering the period 1850–2000 were obtained for USA fertility (Coal 1963) and per capita rate of industrial metabolism (Schurr & Netschert 1960, US Department of Energy 2002).

Mammal masses and annual birth rates were obtained from Ernest (2003). Mammal metabolic rates were estimated from mass using allometric equations for each order (Peters 1983). In humans, annual births per woman were calculated by dividing lifetime fertility by an assumed average 20-year reproductive period. The relationship between fertility and industrial metabolism was determined using ordinary least squares regression of log-transformed variables to be consistent with other allometric calculations. Ten oil-producing nations with extremely high per capita energy production (Oman, Qatar, Saudi Arabia, United Arab Emirates, Bahrain, Kuwait, Netherlands Antilles, Brunei, Libya and Turkmenistan) are significant outliers in most years and are excluded from regression equations.

2.4 RESULTS

Of interest here is the extent to which industrial metabolism constrains human life history and demography. A well-known feature of human ecology is the demographic transition, the tendency of fertility to decline as economic development increases. This phenomenon appears to challenge life-history theory because individuals with greater access to resources have fewer children and apparently reduced biological fitness (Hill & Kaplan 1999, Borgerhoff Mulder 2001). Here we show that per capita fertility is closely correlated to per capita rates of industrial metabolism (E), where E is the individual share of total national energy consumption and includes end consumer uses (heating houses, driving cars, running refrigerators) and per capita contributions to infrastructure (building and maintaining roads, airlines, communications networks and national defense systems).

Figure 2.1 shows that human fertility declines with $E^{-1/3}$ in each time period from 1970 to 1997. Each data point represents the average fertility and per capita power consumption of a nation over the indicated time interval. The qualitative trend in Figure 2.1 is consistent with what is known about the demographic transition: fertility is lower in wealthier nations which have high energy consumption. More compelling is the fact that the allometric exponent (slope of the log–log plot) is statistically indistinguishable from -1/3, as predicted by Equation 3. The same scaling relationship is seen whether fertility is measured as total fertility or crude fertility rate. Although several nations have undergone significant shifts in fertility and energy consumption, the same pattern is apparent in every 5-year time interval since 1970.

A similar dynamic relationship exists across time in the USA from 1850 through 2000, as shown in Figure 2.2. Each data point represents the average fertility rate and *E* for the USA in 5-year intervals. As *E* increases over time, fertility decreases. Again the slope of the regression is statistically indistinguishable from -1/3.

Allometric relationships accurately describe the broad scale pattern of change from pre-industrial averages of 6.5 births per woman and power consumption of 600 W (Livi-Baci 1997) to the modern levels of fertility and power consumption. However, given the short period of available data, the dynamic relationship in most nations is difficult to assess. A 50% decrease in fertility in South Korea is accompanied by a 6-fold increase in *E* (consistent with allometric predictions) while a similar fertility reduction in Cuba occurs with stagnant *E*. Once the allometric relationship is identified, social and economic conditions may explain the residual variation or systematic deviations from the regression line in particular regions, i.e. low fertility in many former Soviet states and high fertility in many oil-producing nations in the Middle East.

Figure 2.3 shows fertility rate as a function of power consumption for modern humans compared with other mammals. The same scaling law with the predicted exponent of -1/3 can account for variation of fertility rate with power consumption, estimated as whole-organism metabolic rate for species of mammals, and nations of humans, where power consumption is estimated as the per capita share of industrial metabolism (*E*). Fertility rates of primates are known to be lower than other mammals (Charnov 1993), and fertility rates of modern humans have decreased from this 'ancestral' primate rate just as predicted by increased power consumption. Figure 2.3

shows that the decline in human birth rates is quantitatively consistent with the life-history patterns of other mammals.

2.5 DISCUSSION

Why should human fertility decisions be guided by industrial metabolism, and why are these patterns quantitatively similar to those observed in primates and other mammals? We hypothesize that parents face a trade off between the number of offspring and the energetic investment in each offspring. Such trade-off decisions have been well explored by biologists, human behavioral ecologists and economists (Smith & Fretwell 1974, Becker & Barro 1988; Kaplan 1996; Mace 1998).

Here we additionally propose that the perceived energetic investment (including material goods and education) required for a child to be competitive in a given society is greater in more consumptive societies. We assume that the cost of a raising a child increases in direct proportion to E. Our assumption is similar to the mammal reproductive allocation assumption made by Charnov (1993). In that model, the observed -1/4 power scaling of reproductive rate with mass results from investing a constant proportion of energetic resources in each offspring.

Finally, we hypothesize that the scaling properties of extra-metabolic networks are similar to biological networks. The scaling of energy delivery rate with network size has been derived for biological networks in terms of mass (West *et al*. 1999), but mass scales linearly with the volume (V) of the metabolic network, i.e. total blood volume (Banavar *et al*. 1999, West *et al*. 1999). Substituting V for mass in the West *et al.* model, the distance (l) and time (t) it takes for a resource to travel from uptake to consumption

(i.e. the distance from the heart to a capillary) scale as $V^{1/4}$ and total energetic rate (E) scales as $V^{3/4}$. Thus,

$$l \sim t \sim E^{1/3} \qquad [2.4]$$

Thus, biological rates are slowed by the increased time it takes to move energetic resources through greater lengths of network in larger organisms. These scaling relationships can be generalized to describe the constraints on the efficiency of any three dimensional transportation network (Banavar *et al*. 1999).

We suggest that in human societies, as in the bodies of organisms, larger networks deliver more energy, but with increased total transport time and infrastructure cost. Some components of this infrastructure are visible networks: oil pipelines, power grids, and rail and highway systems; while other components such as banking systems, governments and research programs may function as virtual networks to develop and spread energy, information and products. If this infrastructure is described by Equation 2.4, the time required to gain energetic resources (E) increases as $E^{1/3}$. Additionally, as E increases, each unit of energy must pass through greater network length (l) incurring increased infrastructure costs.

In our analysis, parents have as many children as they can afford to provision with the energetic resources expected in their society. As the cost and time to obtain these resources increases in more industrialized nations, the number of children parents can support decreases. We propose that the -1/3 power scaling of birth rate reflects the

increasing cost of infrastructure and the increasing time and energy required to collect and distribute greater quantities of resources to children in more industrialized nations.

Given the complexity of the networks supplying E, it may be difficult to determine empirically whether the time and cost of obtaining E increase with $E^{1/3}$ or even to determine the geometry and dimensions of the networks supplying E; however, we suggest that further tests of these hypotheses may be fruitful.

The data show that variation in human fertility rate across nations, through time, and in relation to other mammals, is quantitatively consistent with allometric theory. The cross-national comparison has remained consistent for 30 years, and the dynamic changes in fertility match expectations based on energetic changes in the USA for 150 years. Allometric theory may provide a fruitful framework to link biological and ecological approaches with sociological and economic considerations that may jointly influence human reproduction.

We see our analysis as complementary to other explanations of the demographic transition as the result of ecological and evolutionary processes (Kaplan *et al*. 2002). After socio-economic variables are considered, fertility has been shown to be influenced by population density (Lutz & Qiang 2002) and the diversity of human diseases (Guegan *et al*. 2001). Other social factors—the availability of family planning choices, economic conditions, the unusually high energetic reserves of some nations—may also help to explain the residual variation around the regression lines in Figure 2.1. This analysis is also complementary to other work which seeks to understand the ecological forces which shape human cultures, for example, Collard & Foley (2002).

The products of agriculture, industry and technology are commonly thought to have freed modern humans from energetic and biological constraints. In fact, the limits to human population density, historically imposed by food availability and disease, have greatly increased from less than 1 km^{-2} in pre-agricultural societies to 5–25 km^{-2} in pre-industrial societies (Cipolla 1972, Livi-Baci 1997). The present densities of 30 km^{-2} in the USA and 140 km^{-2} in China far exceed the 4 km^{-2} predicted for a 65-kg mammal (Damuth 1981, Peters 1983). However, limits have been raised, but not removed, and through reliance on new sources of energy and systems of energy acquisition and distribution, humans remain organisms constrained by energy. Per capita energy consumption strongly influences the behavioral and economic decisions that ultimately limit the sizes of families and the investment in rearing children. Recent evidence suggests that the current human population is utilizing natural and industrial systems at levels that are not biologically or energetically sustainable (Wackernagel *et al.* 2002), even as the global population continues to increase in size and resource consumption. Understanding the energetic constraints to population growth and consumption is vital to attaining a globally sustainable human population.

2.6 REFERENCES

Banavar, J.R., Maritan, A. & Rinaldo, A. (1999). Size and form in efficient transportation networks. *Nature*, **399**, 130–132.

Becker, G.S. & Barro, R.J. (1988). A reformulation of the economic theory of fertility. *Q. J. Econ.*, **103**, 1–25.

Borgerhoff Mulder, M. (1998). The demographic transition: Are we any closer to an evolutionary explanation? *Trends Ecol. Evol.*, **13**, 266–270.

Charnov, E.L. (1993). *Life History Invariants*. Oxford University Press, New York.

Cipolla, C.M. (1972). *The Economic History of World Population*. Penguin Books, Baltimore.

Coal, A.J. & Zelnic, M. (1963). *New Estimates of Fertility and Population in the United States*. Princeton University Press, Princeton.

Collard, I.F. & Foley, R.A. (2002). Latitudinal patterns and environmental determinants of recent human cultural diversity: do humans follow biogeographical rules? *Ev. Ecol. Res.*, **4**, 371– 383.

Damuth, J. (1981). Population density and body size in mammals. *Nature*, **290,** 699–700.

Enquist, B.J., Brown, J.H. & West, G.B. (1998). Allometric scaling of plant energetics and population density. *Nature*, **395**, 163–165.

Ernest, S.K.M. (2003). Life history characteristics of placental non-volant mammals. *Ecology,* **84**, 3401 (Ecol. Arch. E084-093).

Guegan, J.F., Thomas, F., Hochberg, M.E., de Meeus, T. & Renaud, F. (2001). Disease diversity and human fertility. *Evolution*, **55**, 1308–1314.

Hill, K. & Kaplan, H. (1999). Life history traits in humans: Theory and empirical studies. *Annu. Rev. Anthropol.*, **28**, 397–430.

Kaplan, H. (1996). A theory of fertility and parental investment in traditional and modern human societies. *Yearb. Phys. Anthropol.*, **39**, 91–135.

Kaplan, H., Lancaster, J.B., Tucker, W.T. & Anderson, K.G. (2002). Evolutionary approach to below replacement fertility. *Am. J. Hum. Biol.*, **14**, 233–256.

Livi-Baci, M. (1997). *A Concise History of World Population*. Blackwell Publishers, Oxford.

Lutz, W. & Qiang, R. (2002). Determinants of human population growth. *Phil. Trans. R. Soc. Lond. B*, **357**, 1197–1210.

Mace, R. (1998). The coevolution of human fertility and wealth inheritance strategies. *Phil. Trans. Roy. Soc. Lond. B*, **353**, 389–397.

Peters, R.H. (1983). *The Ecological Implications of Body Size*. Cambridge University Press, Cambridge.

Schurr, S.H. & Netschert, B.C. (1960). *Energy in the American Economy, 1850–1975*. Johns Hopkins Press, Baltimore.

Smith, C.C. & Fretwell, S.D. (1974). The optimal balance between size and numbers of offspring. *Am. Nat.*, **108**, 499–506.

US Department of Energy (2002). *International Total Primary Energy and Related Information.* http://www.eia.doe.gov/emeu/international/total.html.

Vitousek, P.M., Ehrlich, P.R., Ehrlich, A.H. & Matson, P.A. (1986). Human appropriation of the products of photosynthesis. *Bioscience*, **36**, 368–373.

Vitousek, P.M., Mooney, H.A., Lubchenco, J. & Melillo, J.M. (1997). Human domination of Earth's ecosystems. *Science*, **277**, 494–499.

Wackernagel, M., Schulz, N.B., Deumling, D., Linares, A.C., Jenkins, M., Kapos, V., Monfreda, C., Loh, J., Myers, N., Norgaard, R. & Randers, J. (2002). Tracking the ecological overshoot of the human economy. *Proc. Natl. Acad. Sci. USA*, **99**, 9266–9271.

West, G.B., Brown, J.H. & Enquist, B.J. (1999). The fourth dimension of life: Fractal geometry and allometric scaling of organisms. *Science*, **284**, 1677–1679.

West, G.B., Brown, J.H. & Enquist, B.J. (2000). Scaling in biology: Patterns and processes, causes and consequences. In *Scaling in Biology* (eds. Brown, J.H. & West, G.B.). Oxford University Press, Oxford, 87–112.

West, G.B., Woodruff, W.H. & Brown, J.H. (2002). Allometric scaling of metabolic rate from molecules and mitochondria to cells and mammals. *Proc. Natl. Acad. Sci. USA*, **99**, 2473–2478.

World Resources Institute (2000). *World Resources 2000–01 People and Ecosystems Database*. World Resources Institute, Washington DC.

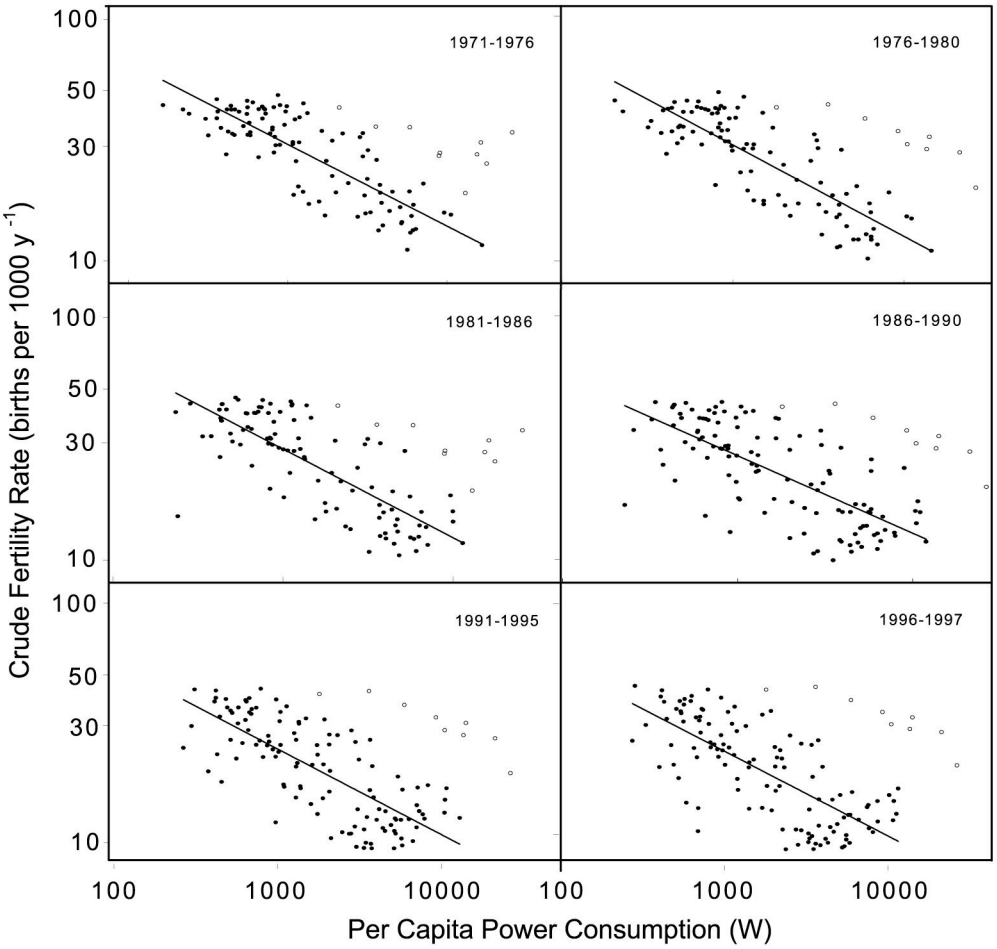

Figure 2.1 Annual human fertility rates (births per 1000 per year) plotted on logarithmic axes as a function of extra-metabolic energy consumption (E) for 98–116 nations in 6 periods from 1971 to 1997. Here infant mortality is subtracted from fertility to more accurately estimate the number of children actually raised by parents. Empty circles represent outliers (all of these nations were major oil producers) not included in the regression. The outliers in the lower left of the middle two panels are Latvia and Bosnia. The slopes of the 6 regressions are between -0.33 and -0.37. These values are statistically indistinguishable from the predicted value of -1/3 ($p > 0.10$ in all cases). The intercepts range from 2.43 to 2.59, with an average r^2 of 61%. Inclusion of outliers, excluding the effect of infant mortality, and considering total fertility rather than annual fertility has little effect on the slope of the relationship.

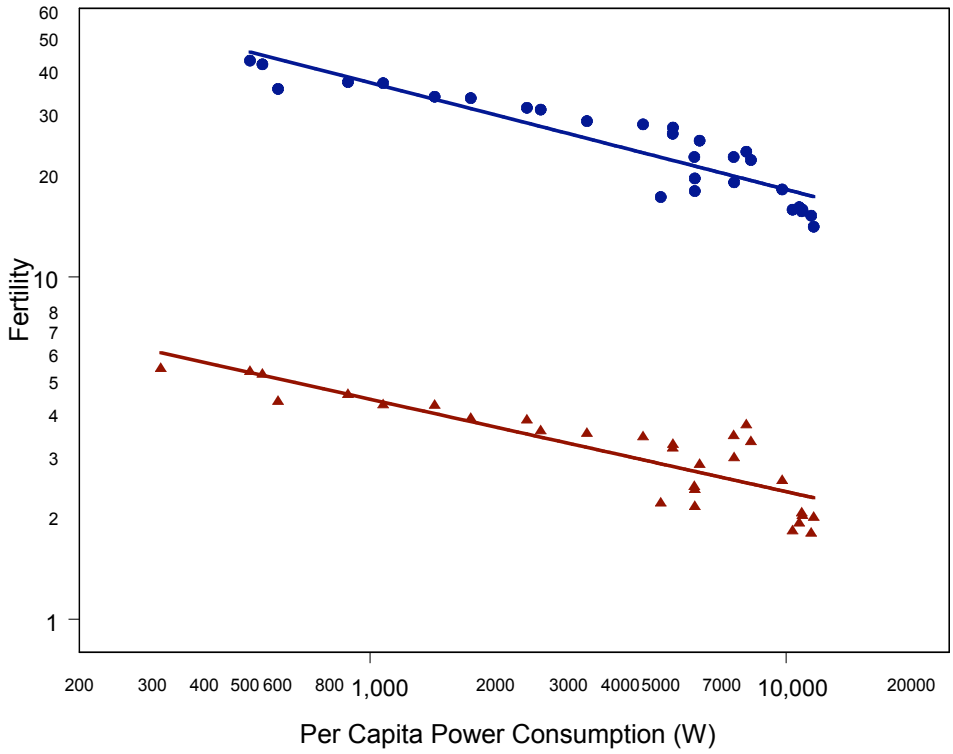

Figure 2.2 Human fertility in the USA as a function of industrial metabolism (E) plotted on logarithmic axes. Data represent five-year intervals from 1850 through 2000. Circles represent crude fertility rate (births per thousand population) and triangles represent lifetime births per woman. The slope for crude fertility is -0.31 ($r^2 = 0.83$) and for total fertility is -0.27 ($r^2 = 0.76$).

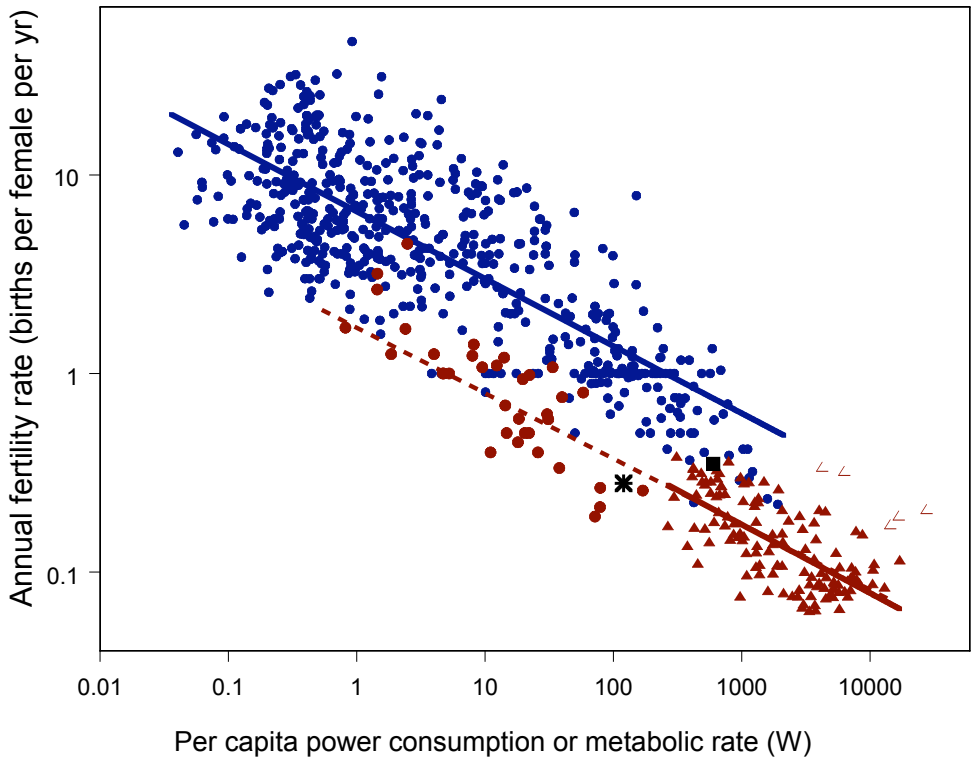

Figure 2.3 Fertility rate of humans and other mammals plotted as a function of power consumption. Power consumption is estimated as metabolic rate for mammals and per capita industrial metabolic rate for humans. Circles represent mammals, with primates in red. Red triangles represent nations and empty triangles are outliers. The black star and box represent human hunter-gathers and pre-industrial agriculturalists, respectively. Fertility was measured as average number of births per female per year of reproductive life for species of mammals and nations of humans using data from 1990 to 1995. Metabolic power (B) of mammals was estimated from body mass using the allometric regression equations for different orders of mammals (Peters 1983). Hunter–gatherer and agriculturalist fertility rates and metabolic consumption are estimated population averages (Livi-Baci 1997). The blue line shows the regression equation for annual fertility of non-primate mammals, $6.54\ B^{-0.339}$ ($r^2 = 0.68$, $p < 0.001$). The red line shows the regression for humans, $1.89\ \mathrm{E}^{-0.346}$ ($r^2 = 0.47$, $p < 0.001$). The dashed line is extended to show the fit through the primate data. The exponent values of -0.339 and -0.346 are well within the 95% confidence intervals for the predicted value of -1/3.

3 An Energetic Exploration of Mammalian Life History: Birth Rate, Reproductive Effort and Offspring Size

3.1 Abstract

Many features of mammal life history scale with body size, while others appear nearly constant across body sizes. I examine the tradeoffs that occur between life history characteristics as mammals allocate energy to reproduction. The consumption and allocation of energy leads to patterns in offspring size, relative reproductive allocation, and birth rates. The analysis suggests a tradeoff between litter size and the interval between litters. When juvenile survivorship is incorporated, the tradeoff is linear. As a result, birth rates are the inverse of time to independence and reproductive allocation is independent of litter size and adult mass.

The time it takes offspring to grow to weaning size appears to follow the predictions of the West, Brown and Enquist (2001) ontogenetic growth model (OGM). The OGM is used to calculate that female mammals allocate approximately 15% of their basal metabolic energy to reproduction. The analysis shows that larger mammals have lower reproductive rates because they spend more time providing energy to grow each offspring. The OGM is incorporated into a fitness model that shows how proportional investment in offspring may maximize parental fitness. The model points to juvenile mortality before and after independence as important factors in determining the optimal size at weaning.

3.2 INTRODUCTION

Many features of mammal life history scale with 1/4 powers of body size. For example, whole-organism metabolism is proportional to mass to the 3/4 power, and birth rate is proportional to mass to the -1/4 power (Peters 1983, Reiss 1989). This paper examines how birth rates are constrained by metabolism. I use life history theory (Charnov 1993) and the West, Brown and Enquist (2001) ontogenetic growth model (OGM) to examine the energetic processes that lead to patterns in offspring size, reproductive allocation, and birth rates. The OGM is based on the allometric scaling of metabolism and body size (Brown *et al.* 2004) and predicts that organism mass increases sigmoidally with time.

Ernest *et al*. (2003) use mammal life history parameters to estimate that biomass production rate (P) scales with mass to the 3/4 power, the same as the scaling of metabolism. Charnov (1993, 2001) finds that the mass of offspring at weaning (M_w) divided by adult mass (M_a) is a constant value, approximately 30% across all mammals. A simple explanation for the scaling of birth rate follows from these two observations. The number of births per unit time (b) is equivalent to the amount of biomass produced per unit time divided by the amount of biomass per offspring. Given that $P \sim M_a^{3/4}$ and $M_w \sim M_a$, if $b = P/M_w$, then $b \sim M_a^{-1/4}$.

The -1/4 scaling of b with M_a hinges on parents rearing offspring to a fixed proportion of adult size. However, it is not known why relative size at weaning is a constant value and why it is about 30%. Offspring could be weaned at some minimum viable size, or they could be under parental care until reaching adult size, as occurs in

altricial birds (Charnov 2002). This paper examines tradeoffs that might lead to a parental care period that lasts until offspring are raised to a consistent proportion of adult size.

I explore what tradeoffs are, and are not, seen as energy is allocated to reproduction. The number of offspring per litter, the relative weaning size (mass at weaning divided by adult mass), the interval between litters, and the time invested in rearing offspring to weaning all affect birth rates and relative reproductive allocation (the percentage of metabolic energy that is allocated to reproduction). Tradeoffs are seen between some of these characteristics, while others appear nearly constant across all mammals.

The analysis gives an estimate of the amount of maternal energy that is devoted to offspring production. Millar (1977) calculates that relative reproductive allocation (R) is slightly higher in small mammals, but he finds most variation in R is due to variation in litter size. Here I estimate that R is approximately constant across mammalian body sizes and litter sizes. The calculation of R may help to elucidate whether maternal energy is diverted from maternal growth, as is suggested by Charnov (2001), or from metabolic scope (West *et al*. 2001, Charnov 1993).

3.3 METHODS

I used data compiled from the literature by Ernest (2003) for adult mass (M_a), mass at weaning (M_w), mass at birth (M_b), litter size at birth (N_b), litters/year, gestation time and post-partum weaning time for 1198 terrestrial eutherian mammal species. Primates, whose life history characteristics are known to deviate from other mammals (Berrigan & Charnov 1993), were excluded. From these variables, I calculated relative weaning size

($\delta = M_w/M_a$), time to weaning (T_w = gestation time + post-partum weaning time), the inter-litter interval (T_I = years/litter) and relative interval between litters ($I_{rel} = T_I/T_w$) which measures the delay between provisioning litters. I also used juvenile mortality rates from Purvis & Harvey (1995) of 47 mammalian species.

I used the theoretical growth equations from the OGM to calculate the time required to grow from conception to the size at weaning in mammals, and I compared those calculations to values in the Ernest dataset. I then used the OGM to calculate the energy used in offspring growth. Finally, I developed a model that demonstrates how intermediate values of relative offspring size can maximize parental fitness.

Statistics were calculated using S-plus 2000 and simulations were done using Matlab Student version 6.5. In all of the regressions, each datum is a species, and each is treated as independent. Least squares (Type 1) regression is used in all cases. Type 1 regression is appropriate when the independent variable is known with greater certainty than the dependent variable, as is the case when mass is the dependent variable (Charnov 1993). Type 1 regression is used throughout this analysis in order to make consistent comparisons between regressions.

T_w and M_w are important variables in the analyses. Weaning is assumed to be a discrete event, although parental provisioning may end gradually. The values in the Ernest dataset are gathered from the literature and likely represent a range of definitions of weaning time and therefore weaning size. This may be an important source of variation in the data.

Another important variable is litter size at the time of weaning. Litter size is usually measured at birth and assumed to be the same at weaning. The effect of juvenile

mortality on weaned litter size is discussed and appears to be important to understanding reproductive tradeoffs.

3.4 RESULTS

The variables used in this analysis are described in Table 3.1. Coefficients and confidence intervals for the regressions between life history characteristics are listed in Table 3.2.

3.4.1 *Allometric Scaling Patterns*

Life history characteristics scale with adult mass (M_a), consistent with results reported elsewhere (Peters 1983, Reiss 1992, Charnov 1993): birth rate (b) scales with $M_a^{-1/4}$; time from conception to weaning (T_w) scales with $M_a^{1/4}$; mass at weaning (M_w) scales with M_a with a slope close to 1 and an intercept of 0.32. Thus, relative size at weaning ($\delta = M_w/M_a$) is nearly constant across mammals and averages 0.32. There is some variation in δ across taxa, and δ tends to decrease with M_a within a clade (Purvis & Harvey 1995).

Biomass production (P_w, measured as weaned biomass per year) scales as $M^{0.67}$. The 95% confidence interval (Table 3.2) excludes the 3/4 scaling expected by Ernest *et al.* (2003). If litter size at weaning is adjusted for pre-weaning mortality (described below), the exponent is raised to 0.71. However, 0.75 is still outside of the 95% confidence intervals of the exponent.

3.4.2 *Tradeoff Between Litter Size and Time Between Litters*

I define the variable I_{rel} as the interval between litters relative to the time from conception to weaning ($I_{rel} = T_I / T_w$). I_{rel} measures the delay or overlap between provisioning litters (Figure 3.1). When $I_{rel} = 1$, gestation of a litter begins as soon as the previous litter is weaned. $I_{rel} > 1$, indicates a delay between weaning one litter and gestation of the next litter. The value of I_{rel} is the number of litters that could theoretically have been weaned sequentially during the interval between litters. $I_{rel} < 1$ indicates that gestation of the next litter begins before the previous litter is weaned.

Since mammals provision their offspring until weaning, it is necessary to know the size of litters at weaning in order to calculate the energy used in reproduction. However, litter size is usually measured at birth. Litter size at birth (N_b) is an overestimate of weaned litter size (N_w) if there is any mortality during the parental care period. It is a biased estimate if there is differential mortality in large litters.

I use juvenile mortality data to estimate N_w from N_b. Data from Purvis & Harvey (1995) show a significant decline in survival to maturity (S_α) as N_b increases ($S_\alpha = -0.436\ N_b^{-0.32}$, $r^2 = 0.25$, $n = 47$, $p < 0.001$). Promislow & Harvey (1990) also find a significant correlation between juvenile mortality rate and N_b, even when controlling for adult mortality.

Juvenile mortality may be different during the period of parental care and after parental care, so the rate of survival to maturity does not translate exactly to the rate of survival to weaning. However, if there is increased mortality in larger litters, it likely

occurs prior to weaning when large litters present the maximal energetic cost to the mother. Assuming that survival to weaning shows the same scaling with litter size as survival to maturity, I estimate that N_w equals N_b multiplied by the juvenile survival rate calculated from Purvis & Harvey: $N_w \sim S_\alpha N_b \sim N_b^{0.68}$.

N_b and I_{rel} both vary with body size (Figure 3.2) and with each other (Figure 3.3a). N_b and I_{rel} are more correlated with each other than they are with body size (Table 2). There is also a strong positive correlation between I_{rel} and N_w (Figure 3.3b). The 95% confidence interval for the slope of the regression includes 1, and the 95% confidence interval for the intercept includes 0 (Table 2), indicating a 1:1 tradeoff between N_w and I_{rel}. When $N_w = 1$, $I_{rel} = 1$. When a litter of size N_w is weaned, the mother waits a period of $N_w T_w$ to begin the next litter. This indicates that the rate at which offspring are weaned is not affected by N_w.

Since b is the product of N_b and litters per year, the tradeoff between N_b and I_{rel} generates b nearly proportional to T_w^{-1} (Figure 3.4, Table 3.2). Although the residuals of the regression of b on T_w are significantly correlated with N_b ($F = 64.02$, $n = 401$, $p < 0.001$), b is very close to the inverse of T_w across all species.

3.4.3 *Testing the Ontogenetic Growth Model*

The OGM predicts that mass follows a sigmoidal curve with time defined by $dm/dt = am^{3/4} - b_1 m$, where a is a scaling constant based on the energy to create and maintain cells and is estimated to be $91 g^{1/4} yr^{-1}$ for mammals, $b_1 = aM^{-1/4}$, and M is maximum attainable mass of a species. The OGM assumes that observed adult size (M_a) equals M. The growth equation can be integrated to find the time it takes to reach size δ (Figure 3.5a).

$$T_w = -4\ln(1-\delta^{1/4})/(aM^{-1/4}) \qquad [3.1]$$

Observed weaning times can be compared to the OGM prediction for weaning time (Equation 3.1). The prediction shows a 1:1 correspondence with the data, and the regression explains 69% of the variance (Figure 3.6a). Residuals from the regression are not correlated with N_b ($F = 0.994$, $n = 297$, $p = 0.341$). Equation 3.1 can also be used to predict gestation time if relative size at birth is substituted for δ. The regression between predicted and observed gestation time is also significant ($r^2 = 0.85$, $n = 602$, $p < 0.001$), but observed gestation times are about 20% longer than predicted by Equation 3.1 (Figure 3.6b).

3.4.4 *Energy for Growth and Relative Reproductive Output*

If offspring grow according to the OGM, one can calculate the amount of energy each offspring uses to grow to size δ and the percent of maternal energy that is allocated to reproduction (R, Figure 3.5b). The calculation of R assumes offspring grow via the OGM, weaning is a discrete event, and all maternal provisioning occurs via lactation. To simplify the calculations, initially assume $N_b = 1$ and $I_{rel} = 1$. $N_b > 1$ is discussed below.

Appendix 3.7 shows calculations of the energy required to grow from conception to weaning (E_w).

$$E_w = ME_c/m_c\,(-4\ln(1-\delta^{1/4}) - 4\delta^{1/4} - 2\delta^{1/2} - 4/3\delta^{3/4}) \qquad [3.2a]$$

E_c and m_c are metabolic constants describing the energy to create a cell and the mass of a cell. They are assumed constant for all mammals and are estimated in the OGM. Thus, the energy required to grow to size δ varies only as a function of maximum size (M) and δ.

The metabolic energy expenditure of the mother (E_m) can be integrated over the parental care period. Maternal basal metabolic rate $B = B_0 M^{3/4}$. B_0 is a scaling constant for mammals such that $B_0 = a\,(E_c / m_c)$. Since the period of offspring growth to size δ is T_w, maternal metabolic energy expended over the parental care period is $E_m = BT_w$. Using Equation 3.1 for T_w,

$$E_m = -4\ln(1-\delta^{1/4})\, ME_c/m_c \qquad [3.3a]$$

Relative reproductive effort (R) can be calculated as the percentage of maternal metabolism that is allocated to reproduction so that $R = E_w / E_m$.

$$R = \frac{-4\ln(1-\delta^{1/4}) - 4\delta^{1/4} - 2\delta^{1/2} - 4/3\delta^{3/4}}{-4\ln(1-\delta^{1/4})} \qquad [3.4a]$$

R is independent of the scaling constants and adult mass, and is only a function of δ. E_w, E_m and R are shown as functions of δ in Figure 3.7. When $\delta = 0.32$, Equation 3.4a gives $R = 0.15$. Thus, Equation 3.4a predicts that 15% of maternal metabolism is allocated to growing offspring.

The calculations of R, E_w, and E_m are based on mammals for which $N_b = 1$ and $T_I = T_w$. The calculations can be generalized for $N_b > 1$. The energy to raise a litter of size N_w is $E_{w\text{-}lit} = N_w E_w$. When $N_w > 1$, then $T_I > T_w$. Maternal energy available for reproduction can be integrated from the time one litter is conceived until the time the next litter is conceived (T_I). Integrating over T_I implies that maternal energy is stored or replenished during periods in which she is not directly provisioning offspring. Then $E_{m\text{-}lit} = BT_I$ and $R_{lit} = (N_w E_w) / (BT_I)$. This calculation of R_{lit} is shown as a function of M_a for the species in the Ernest data (Figure 3.8). R_{lit} ranges from 0.02 to 0.54 with a mean of 0.16 (95% CI = 0.16 ± 0.01). There is no significant effect of M_a on R_{lit} (F =1.07, n = 229, p = 0.301); nor is there an effect of N_b on R_{lit} (F = 2.0, n = 229, p = 0.159).

Since maternal energy (E_w) is integrated over the inter-litter interval (T_I), and larger litters are associated with proportionally larger T_I (Figure 3.3b), the reproductive effort to raise a litter is independent of litter size. Thus, $R_{lit} = R$.

3.4.5 *Reproductive Energy Diverted from Growth*

The OGM assumes that the mass of an adult (M_a) is equal to maximum mass (M), which is the size where maintenance energy equals metabolic intake. Thus, reproduction is fueled from metabolic scope—the difference between field and basal metabolic rate. Alternatively, Charnov (2001) suggests that reproductive energy is diverted from growth; mammals stop growing at some proportion μ of M, and the energy for reproduction equals metabolism at size μM minus maintenance metabolism at size μM (Figure 3.9).

If μ <1, the calculations for E_w, E_m and R change. Previously, δ was calculated as M_w/M_a based on the assumptions that μ =1 and $M_a = M$. However, if, as according to Charnov (2001) $M_a = \mu M$, then we can define a term, δ_1, for offspring size relative to the theoretical maximum mass (M) in the OGM: $\delta_1 = \mu\delta$. New equations for E_w, E_m and R are obtained by substituting δ_1 for δ and μM for M_a:

$$E_w = ME_c/m_c\,(-4\ln(1-\delta_1^{1/4}) - 4\delta_1^{1/4} - 2\,\delta_1^{1/2} - 4/3\delta_1^{3/4}) \qquad [3.2b]$$

$$E_m = \mu^{3/4}ME_c/m_c\,(-4\ln(1-\delta_1^{1/4})) \qquad [3.3b]$$

$$R = E_w/E_m = ((-4\ln(1-\delta_1^{1/4}) - 4\delta_1^{1/4} - 2\,\delta_1^{1/2} - (4/3)\,\delta_1^{3/4}))/(-4\ln(1-\delta_1^{1/4})\,\mu^{3/4}) \qquad [3.4b]$$

Charnov (2001) uses a dimensional approach to estimate that $\mu = 0.7$. He further calculates that the maternal energy that is diverted from growth to reproduction is

$E_{rep} = [\ 1 - \mu^{1/4}]\ E_m$ (Figure 3.9b). If μ is set such that all reproductive energy is diverted from growth, then E_{rep} must equal E_w. Given that the empirical value of $\delta = 0.32$ (Ernest 2003), then $E_{rep} = E_w$ when $\mu = 0.54$. This estimate of μ is significantly different from $\mu = 0.7$ ($t = -15.02$, $n = 229$, $p < 0.001$).

R is not sensitive to the different predicted values of μ. Equation 3.4b gives $R = 0.15$ for $0.7 < \mu < 1$. If $\mu = 0.54$, $R = 0.14$. Thus, regardless of whether reproduction is fueled by metabolic scope or from energy diverted from growth, relative reproductive effort is approximately 15%.

3.4.6 *Optimal Relative Size at Weaning*

If offspring growth from conception to weaning is described by the OGM, then the OGM can be used to model maternal fitness as a function of δ. Fitness of the mother (W) is the product of birth rate (b), survival to maturity (S_α) and expected adult lifespan (Charnov 1993). Assuming that δ does not affect maternal lifespan, then $W \sim bS_\alpha$.

Across species $b = T_w^{-1}$ (Figure 3.4) because of the tradeoff between N_w and I_{rel}. I assume that $b = T_w^{-1}$ within species as well as between species so that:

$$W \sim S_\alpha / T_w \qquad [3.5]$$

T_w is a function of δ (Equation 3.1.), and S_α can also be defined as a function of δ. Assume pre-weaning mortality rate (Z_1) is constant with respect to δ. Assume that parental care ends at weaning so that post-weaning juvenile mortality is greater than pre-

weaning mortality. Also assume that post-weaning mortality rate is a function of mass (and also of time, since mass changes over time), so that the shape of mortality looks something like that shown in Figure 3.10. Define Z_2 as the average mortality rate from T_w (which is determined by δ in Equation 3.1) to the time at which maturity is reached (T_α). Z_2 will decrease as δ increases because mortality will be averaged over a period in which mass is greater.

The particular functions for Z_1 and Z_2 are unknown. Purvis & Harvey (1995) suggest that juvenile and adult mortality scale as $M^{-1/4}$, so set $Z_1 = M^{-1/4}$ assuming the scaling pre-factor is 1. Z_1 is constant within a species but scales with mass across species. Set $Z_2 = pZ_1\delta^{-q}$ where $p > 1$ and $q > 0$, so that initially Z_2 is greater than Z_1, but Z_2 decreases with δ. S_α equals survival from 0 to T_w multiplied by survival from T_w to T_α: $S_\alpha = \exp(-Z_1T_w)\exp(-Z_2(T_\alpha - T_w))$. Rearranging terms gives:

$$S_\alpha = \exp[(Z_2-Z_1)T_w - Z_2T_\alpha] \qquad [3.6]$$

Substituting Equation 3.6 into Equation 3.5 gives:

$$W \sim \exp[(Z_2-Z_1)T_w - Z_2T_\alpha] / T_w \qquad [3.7]$$

where $T_w = -4\ln(1-\delta^{1/4})/(aM^{-1/4})$

For any given species, a, M, T_α are constants given by the OGM. Thus, W varies only as a function of δ, Z_2 and $(Z_2 - Z_1)$.

The asymptotic shape of the OGM growth curve can generate an intermediate δ that maximizes W. Equation 3.1 enables calculating T_α. Since the OGM growth curve is asymptotic, maximum mass (M) is never reached. I assume M_a is 95% of M, so 0.95 is substituted for δ in Equation 3.1. (Note that if $\mu<1$ then μ should be substituted for δ). W is calculated with simulations since there is no explicit solution for maximizing W as a function of δ. By substituting $a = 91 g^{1/4} yr^{-1}$ and choosing M = 1000 g, p = 4 and q = 0.5 in Equation 3.7, then b, Z_2, S_α and W can be shown as functions of δ (Figure 3.11). In this case, W is maximum when δ is 0.4.

The optimal relative size at weaning that maximizes fitness is invariant with respect to mass. In the simulations, optimal δ increases as p and q increase. The variable p indicates the increase in mortality once parental care ends, and q indicates the degree of size dependence of mortality after weaning. Thus, the height and shape of the post-weaning juvenile mortality function determine the relative weaning size that maximizes fitness.

3.5 DISCUSSION

The results show that the proportion of maternal metabolism given to offspring and the relative size at weaning are invariant with respect to adult mass in mammals (Figure 3.8), but there are differences in energy allocation. Smaller mammals have slightly larger litters and longer relative inter-litter intervals (Figure 3.2). There is a tradeoff between litter size and the amount of time between weaning one litter and conceiving the next. The time and energy required to grow to the size at weaning can be

calculated by the OGM. A fitness model which incorporates ontogenetic growth shows that intermediate relative weaning sizes can maximize fitness.

The tradeoff between litter size and the interval between litters is evident only when the interval between litters is measured relative to weaning time. That is, a small mammal with a large litter may have a short delay between litters if measured in number of days between litters, but a long delay relative to the time spent providing care for each litter. For example, the rodent *Sigmodon hispidus* has 2 litters each year while *Equus zebra* has only one litter every year and a half. However, when measured relative to weaning time, I_{rel} for the rodent is 4.34 while I_{rel} for the zebra is 0.9. The tradeoff between N_w and I_{rel} illustrates the importance of rescaling variables of interest by biological time. Once the effect of body size (and its effect on T_w) has been accounted for, one can examine other biologically interesting tradeoffs (Brown *et al.* 2004).

The delay between litters increases in proportion to litter size once increased juvenile mortality in large litters is accounted for. Thus, a mammal of a given size produces a similar number of offspring per year regardless of whether they are in large, widely spaced litters or in small litters that are born close together.

This tradeoff suggests that mammals that have large litters are capital breeders, storing or replenishing energy in the time between provisioning litters. Mammals with smaller litters may be considered income breeders that are constantly allocating energy to provision a small litter. Regardless of which strategy is used, the time it takes to provision offspring with energy limits the rate at which offspring can be produced. Larger mammals, which provide more energy to each offspring, space their offspring further apart.

Since the energetic demands of offspring are highest just before weaning, mothers with small litters may store energy early in gestation so that it may be expended later in lactation. It should be interesting to see what role seasonality plays in the tradeoff between litter size and the inter-litter interval. One might expect mammals that live in highly seasonal environments to space their litters to correspond with favorable seasons. These mammals would be predicted to have larger litters that are spaced further apart. Larger litters in more seasonal environments are consistent with the findings of Millar & Innes (1985) that litter size in Peromyscus maniculatus increases with both latitude and elevation.

The OGM accurately predicts time to weaning (Figure 3.6a). In the OGM, the rate at which energy is converted to growth is controlled only by mass relative to maximum mass. Since offspring growth trajectories follow the OGM, there is an implication that offspring growth rates are limited primarily by their own abilities to assimilate energy rather than by the maternal supply of energy. In other words, once mothers supply sufficient energy to their offspring, the offspring grow themselves according to the OGM, and additional maternal energy does not speed growth any further.

Interestingly, gestation times are more strongly correlated with model predictions than are post-partum weaning times; however, gestation times are consistently underestimated by the OGM by about 20% (Figure 3.6b). This could be explained if maternal energy supply were limiting growth *in utero*. McNab (1980) found that mammals with higher energy intake rates for their size have offspring with higher growth rates. Pregnant mammals might not be able to supply sufficient energy to maximize offspring growth if they are allocating resources to other activities such as defense and

resource acquisition. However, one might expect maternal energy supply to be most limiting when litter size is larger, but there is no correlation between litter size and the residuals of the OGM predictions. Maternal energy supply may not limit growth in large litters if energy is stored in the interval between litters, as is implied by the tradeoff between N_w and I_{rel}.

In the cross-species analysis, there does not appear to be a correlation between litter size and relative size at weaning ($F = 1.257$, $n = 334$, $p = 0.263$). This is interesting since many studies report a tradeoff between litter size and offspring size within species or between species when adult mass is held constant, e.g., Millar (1986).

In this analysis, mothers allocate approximately 15% of their metabolism to growing offspring throughout their reproductive lives. The calculation of reproductive effort does not determine whether this energy is diverted from growth or from metabolic scope. However, it does suggest a testable hypothesis. If all reproductive energy is diverted from growth, then this analysis predicts not only that μ is constant across all mammals, as predicted by Charnov (2001), but also that $\mu = 0.54$ which is lower than Charnov's prediction of $\mu = 0.7$. The value of μ changes the size of fastest growth rate relative to adult mass (M_a). Growth rate is fastest at $0.32M$, where M is the theoretical maximum mass predicted by the OGM. Since $\mu = M_a/M$, Charnov predicts that the point of fastest growth is at $0.45M_a$; this analysis predicts it at $0.57M_a$, and the OGM predicts it at $0.32M_a$. Initial examination of growth curves in the literature indicates that distinguishing among these hypotheses may be difficult.

The OGM appears to describe growth trajectories from conception to weaning. The asymptotic shape of the growth curve can generate an intermediate optimal size at

weaning that maximizes parental fitness (W) which is proportional to bS_α. b declines sharply as δ increases when δ is small, but the decline in b tapers off as δ becomes large (Figure 3.11). Thus, many S_α functions that are nearly linear with δ will have a more shallow slope than b for small δ, but a steeper slope than b for large δ. These conditions produce a W that is maximized when δ is an intermediate value. It remains an open question to specify biologically realistic functions for S_α and juvenile mortality that produce an intermediate optimum δ.

Female mammals face a trade off between investing in existing offspring and conceiving a new litter. The fact that δ (measured relative to M_a) is consistently near 0.3 suggests that it represents an optimal allocation decision by the mother. The model developed here generates an intermediate optimal δ while other life history models have not. The model points to the difference in juvenile mortality before and after weaning as important life history parameters. The approach used here may begin to explain why parental investment in mammals stops after offspring reach a fixed proportion of adult size.

3.6 References

Berrigan, D. & Charnov, E.L. (1993). Phylogenetic contrasts and the evolution of mammalian life histories. *Evol. Ecol.*, **7,** 270-278.

Brown, J.H., Gillooly, J.F., Allen, A.P., Savage, V.M. & West, G. B. (2004). Toward a metabolic theory of ecology. *Ecology,* **85**, 1771-1789.

Charnov, E.L. (1993). *Life History Invariants*. Oxford University Press, Oxford, UK.

Charnov, E.L. (2001). Evolution of mammal life histories. *Ev. Ecol. Res.*, **3**, 521-535.

Charnov, E.L. (2002). Reproductive effort, offspring size and benefit–cost ratios in the classification of life histories. *Ev. Ecol. Res.*, **4,** 749-758.

Ernest, S.K.M., Enquist, B.J., Brown, J.H., Charnov, E.L., Gillooly, J.F., Savage, V.M., White, E.P., Smith, F.A., Hadly, E.A. & Haskell, J.P. (2003). Thermodynamic and metabolic effects on the scaling of production and population energy use. *Ecol. Lett.,* **6**, 990-995.

Ernest, S.K.M. (2003). Life history characteristics of placental non-volant mammals. *Ecology,* **84**, 3401 (*Ecol. Arch.* E084-093).

McNab, B.K. (1980). Food habits, energetics and the population biology of mammals. *Am. Nat.,* **116**, 106-124.

Millar, J.S. (1977). Adaptive features of mammalian reproduction. *Evolution,* **31,** 370-386.

Millar, J.S. (1986). Pre-partum reproductive characteristics of eutherian mammals. *Evolution,* **35,** 1149-1163.

Millar, J.S. & Innes, D.G.L. (1985). Breeding by *Peromyscus* over an elevational gradient. *Can. J. Zool.,* **63,** 124–129.

Peters, R.H. (1983). *The Ecological Implications of Body Size.* Cambridge University Press, Cambridge, UK.

Promislow, D.E.L. & Harvey, P.H. (1990). Living fast and dying young: A comparative analysis of life history variation among mammals. *J. Zool.,* **220,** 417-437.

Purvis, A. & Harvey, P.H. (1995). Mammal life-history evolution: A comparative test of Charnov's model. *J. Zool.,* **237,** 259-283.

Reiss, M.J. (1989). *The Allometry of Growth and Reproduction.* Cambridge University Press, Cambridge, UK.

Sibly, R.M., Collett, D., Promislow, D.E.L, Peacock, D.J. & Harvey, P. H. (1997). Mortality rates in mammals. *J. Zool.,* **243,** 1-12.

West, G.B, Brown, J.H. & Enquist, B.J. (2001). A general model for ontogenetic growth. *Nature,* **413,** 628-631.

3.7 APPENDIX: CALCULATIONS OF OFFSPRING ENERGY REQUIREMENTS

The metabolism used for maintenance and growth of an organism is $B = B_0 m^{3/4}$. Assume that mass changes according to the West *et al*. ontogenetic growth model. Then the total energy used by offspring during the parental care period (E_w) is integrated from the mass at conception to the mass at weaning.

$$E_w = \int_0^{T_w} T_w B_0 (m_t)^{3/4}\, dt \qquad [3.8]$$

From the growth model: $dm/dt = am^{3/4} - bm$. Assuming $m_t \approx 0$ at $t = 0$ then mass at time t is described by:

$$m_t = [(a/b)\ (1\text{-}e^{-bt/4})]^4 \qquad [3.9]$$

Substituting Equation 3.9 into Equation 3.8 gives:

$$E_w = \int_0^{T_w} B_0 ((a/b)^4\ (1\text{-}e^{-bt/4})^4)^{3/4}\, dt$$

$$= B_0(a/b)^3 \int_0^{T_w} (1\text{-}e^{-bt/4})^3\, dt$$

$$= B_0(a/b)^3 \int_0^{T_w} (1\text{-}3e^{-bt/4}+3e^{-bt/2}\text{-}e^{-3bt/4})\, dt$$

$$= B_0(a/b)^3 \quad [T_w + 12/b(e^{-b\,T_w/4}\ \text{-}1)\ \text{-}6/b(e^{-b\,T_w/2}\ \text{-}\ 1) + 4/(3b)\ (e^{-3b\,T_w/4}\ \text{-}\ 1)]$$

Substituting $T_w = -4\ln(1- \delta^{1/4})/b$

$$= B_0(a/b)^3\ [-4\ln(1- \delta^{1/4})/b + 12/b(e^{\ln(1-\delta 1/4)}\text{-}1)\ \text{-}\ 6/b(e^{2\ln(1-\delta 1/4)}\text{-}\ 1) + 4/(3b)\ (e^{3\ln(1-\delta 1/4)}\text{-}1)]$$

Simplifying:

$$= B_0(a/b)^3\ b^{-1}\{-4\ln(1- \delta^{1/4}) + 12((1- \delta^{1/4})\text{-}1)\ \text{-}6[(1- \delta^{1/4})^2\text{-}1] + 4/3[(1- \delta^{1/4})^3\text{-}1)]\}$$

Substituting $B_0 = aE_c/m_c$ and expanding terms:

$$= E_c/m_c\,(a/b)^4\ \{-4\ln(1- \delta^{1/4}) + 12(-\ \delta^{1/4})\ \text{-}6\ [(1- 2\delta^{1/4} + \delta^{1/2})\ \text{-}1]$$
$$+ 4/3[(1- 2\delta^{1/4} + \delta^{1/2}\text{-}[\delta^{1/4}\ \text{-}2\delta^{1/2} + \delta^{3/4}]\text{-}1)]\}$$

Simplifying and substituting $M = (a/b)^4$ gives

$$E_w = E_c/m_c M\,[-4\ln(1- \delta^{1/4})\ \text{-}\ 4\delta^{1/4}\ \text{-}2\delta^{1/2}\ \text{-}\ 4/3\delta^{3/4}] \qquad [3.10]$$

Table 3.1 Definitions of life history variables

Variable	Definition	Source or calculation
A	Metabolic scaling constant in the OGM	$91 g^{1/4}$ per year from West *et al.* (2001)
B	Organism metabolic rate	$B = B_0 M^{3/4}$
B_0	Metabolic scaling constant	West *et al.* (2001)
B_1	Metabolic maintenance constant in the OGM	West *et al.* (2001)
b	Birth rate (births per year)	$b = N_b$ (litters/year)
δ	Relative size at weaning	M_w/M_α
E_c	Energy to create a cell in the OGM	West *et al.* (2001)
E_m	Metabolic energy of the mother	$E_m = -4ME_c/m_c \ln(1- \delta^{1/4})$
E_{rep}	Energy for reproduction diverted from growth	$[1 - \mu^{1/4}] E_m$
E_w	Energy required to grow to size δ	$E_w = ME_c/m_c (-4\ln(1- \delta^{1/4}) - 4\delta^{1/4} -2\delta^{1/2} - 4/3\delta^{3/4})$
I_{rel}	Time between litters relative to weaning time	$I_{rel} = T_1/T_w$
N_b	Litter size at birth	Ernest (2003)
N_w	Litter size at weaning, adjusted for mortality	$N_w = N_b^{0.68}$
M	Maximum attainable mass	West *et al.* (2001)
M_a	Observed adult size	Ernest (2003)
M_b	Mass at birth	Ernest (2003)
M_w	Mass at weaning	Ernest (2003)
m_t	Mass as a function of time in the OGM	West *et al.* (2001)
m_c	Mass of a cell	West *et al.* (2001)
μ	Adult size relative to maximum size	$\mu = M_a/M$
P	Biomass production rate (based on N_b)	$P = M_b N_b$ (litters/year)
P_w	Weaned Biomass Production Rate	$P_w = M_w N_w$ (litters/year)
R	Relative Reproductive Effort	$R = E_w/E_m$
S_α	Survival to size at maturity	$S_\alpha = \exp[((Z_2-Z_1)*T_\delta) - Z_2 T_\alpha]$
T_1	Time between birth of each litter	years/litter from Ernest (2003)
T_w	Time from conception to weaning	Empirical data from Ernest (2003) Predicted by the OGM: $T_w = -4\ln(1-\delta^{1/4})/(aM^{1/4})$
W	Fitness	$W \sim \exp[((Z_2-Z_1)*T_w) - Z_2 T_\alpha] / T_w$
Z_1	Juvenile mortality prior to weaning	$Z_1 = M^{1/4}$
Z_2	Juvenile mortality after weaning	$Z_2 = pZ_1\delta^{-q}$ where $p > 1$, $0 < q < 1$
Z_3	Adult mortality	$Z_3 \sim M^{1/4}$

Table 3.2 Regression statistics of life history variables[a]

	Intercept	*Intercept 95% CI*	Slope	Slope 95% CI	r^2	*N*
b vs M_a	1.39	1.34 to 1.45	-0.26	-0.28 to -0.24	0.64	548
M_w vs M_a	-0.33	-0.38 to -0.27	0.93	0.92 to 0.95	0.97	339
T_w vs M_a	-1.24	-1.27 to -1.21	0.24	0.23 to 0.25	0.83	575
P vs M_a	1.13	1.04 to 1.22	0.67	0.64 to 0.69	0.91	247
P_w vs M_a	0.84	0.76 to 0.92	0.71	0.69 to 0.74	0.93	247
T_l vs M_a	0.70	0.65 to 0.76	-0.12	-0.14 to -0.11	0.39	393
N_b vs M_a	0.77	0.74 to 0.80	-0.13	-0.14 to -0.12	0.42	1065
I_{rel} vs N_b	0.03	0.00 to 0.07	0.66	0.59 to 0.73	0.46	401
I_{rel} vs N_w	0.03	0.00 to 0.07	0.97	0.87 to 1.07	0.46	401
S_a vs N_b	-0.37	-0.44 to -0.17	-0.32	-0.48 to -0.19	0.25	47
b vs T_w	0.17	0.09 to 0.25	-1.08	-1.02 to -1.14	0.78	401

[a] All variables are $\log_{10}$ transformed. Least squares (Type 1) regression is used. The intercept indicates the scaling pre-factor, the slope of the regression indicates the scaling exponent and *N* indicates the number of species in the regression. All regressions are significant (p <0.001).

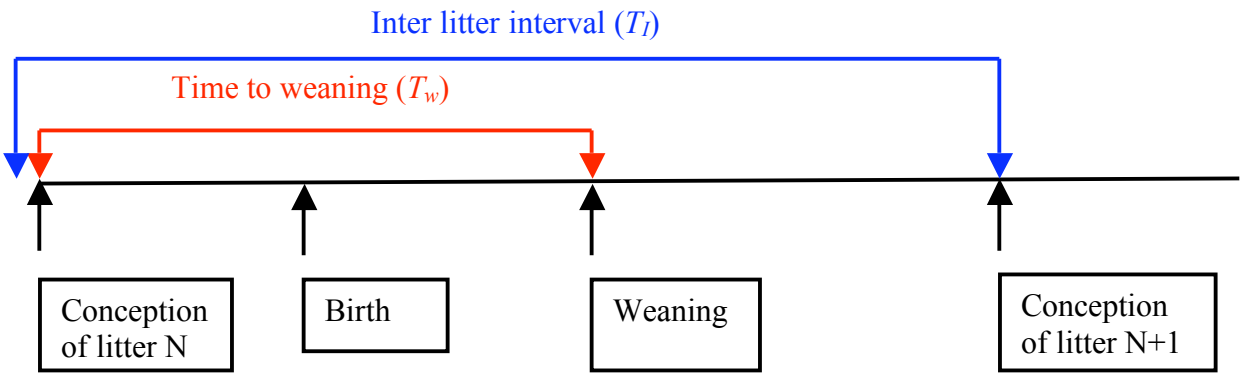

Figure 3.1 Events that delineate the time to weaning and inter litter interval. The relative time between litters (I_{rel}) equals T_I / T_w. Here the time to wean the $N^{\underline{th}}$ litter is less than the interval between litters, so $I_{rel} > 1$.

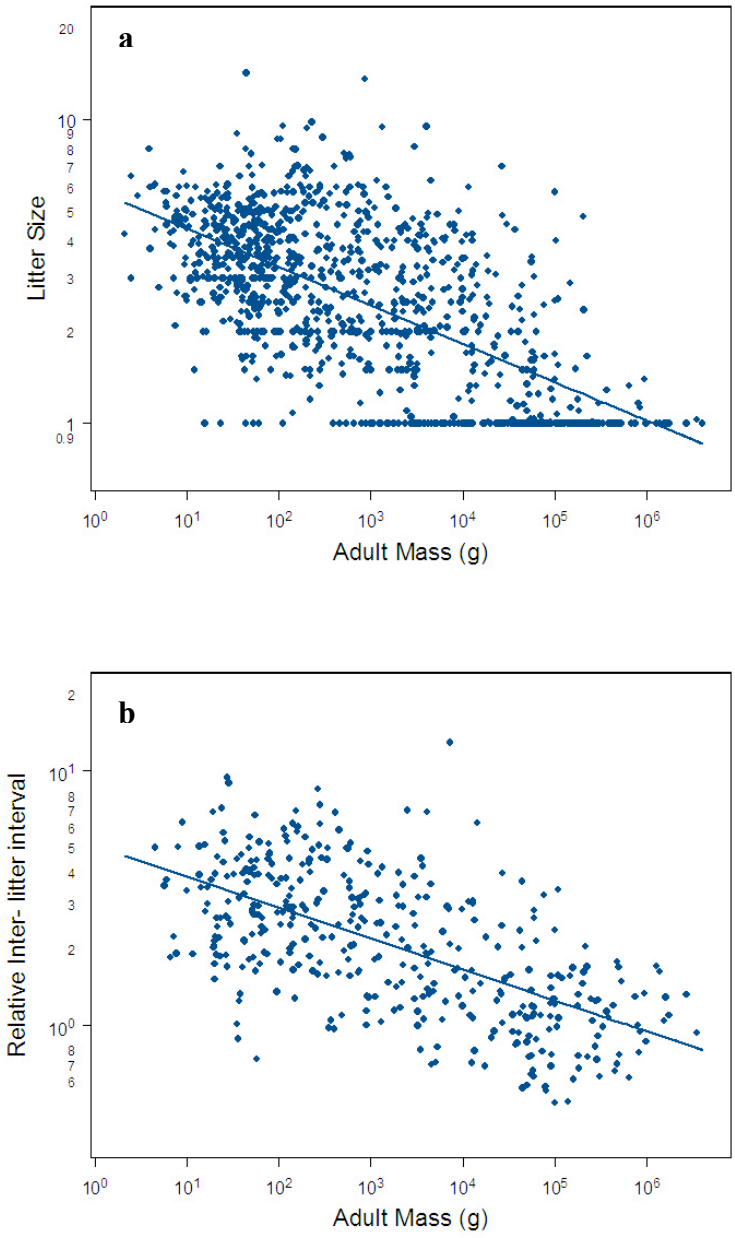

Figure 3.2 Litter size and relative time between litters as a function of adult mass. **(a)** Litter size at birth (N_b) as a function of adult mass (M_a). Regression statistics appear in Table 2. **(*b*)** Relative time between litters I_{rel} as a function of adult mass (M_a). $I_{rel} > 1$, indicates a delay between weaning one litter and gestation of the next litter. $I_{rel} < 1$ indicates that the next litter is conceived before the previous litter is weaned. Regression statistics appear in Table 2.

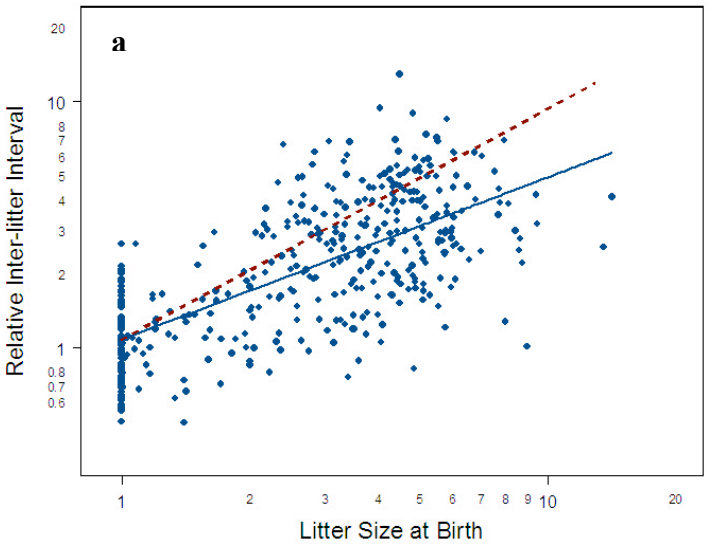

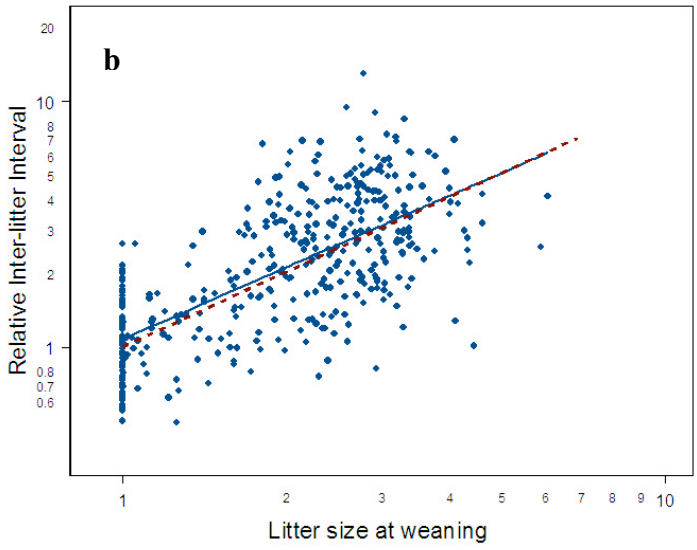

Figure 3.3 Relative time between litters as a function of litter size.
(a) Relative time between litters I_{rel} as a function of litter size at birth (N_b).
The dashed line is the 1:1 line and the solid line is the regression line. Regression statistics appear in Table 2. ***(b)*** Relative time between litters I_{rel} as a function of estimated litter size at weaning (N_w). N_w equals N_b at birth adjusted by juvenile survival rate that scales with $N_b^{0.32}$, from data reported in Purvis & Harvey (1995). The dashed line is the 1:1 line and the solid line is the regression line which is indistinguishable from the 1:1 line. Regression statistics appear in Table 3.2.

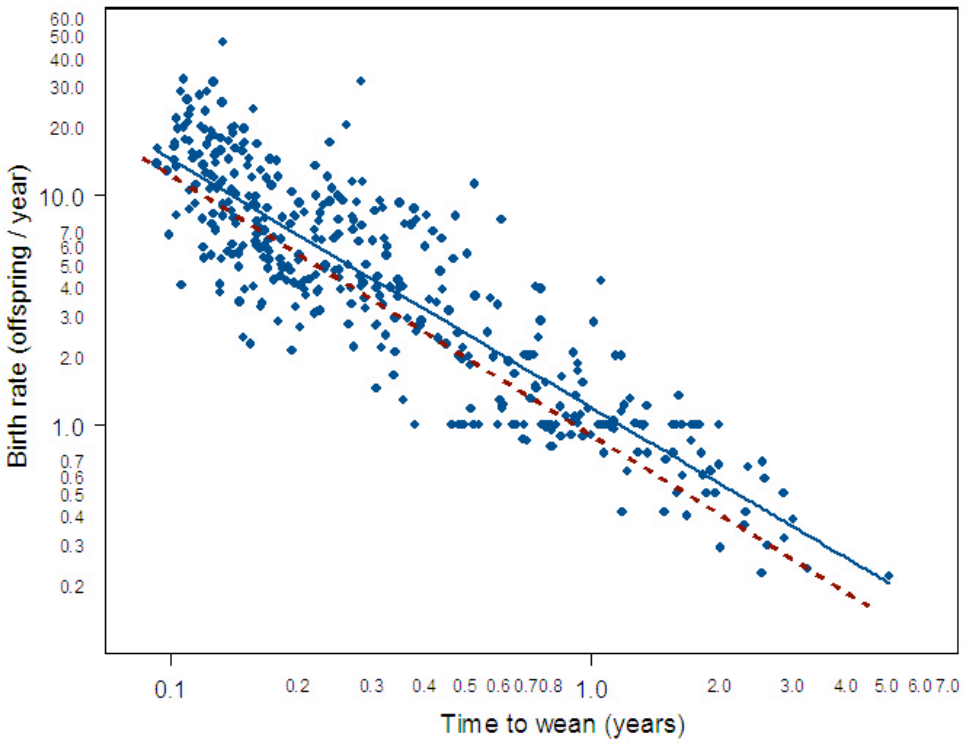

Figure 3.4 Birth rate versus time to weaning. The dashed line is the -1:1 line and the solid line is the regression line. Regression statistics appear in Table 2.

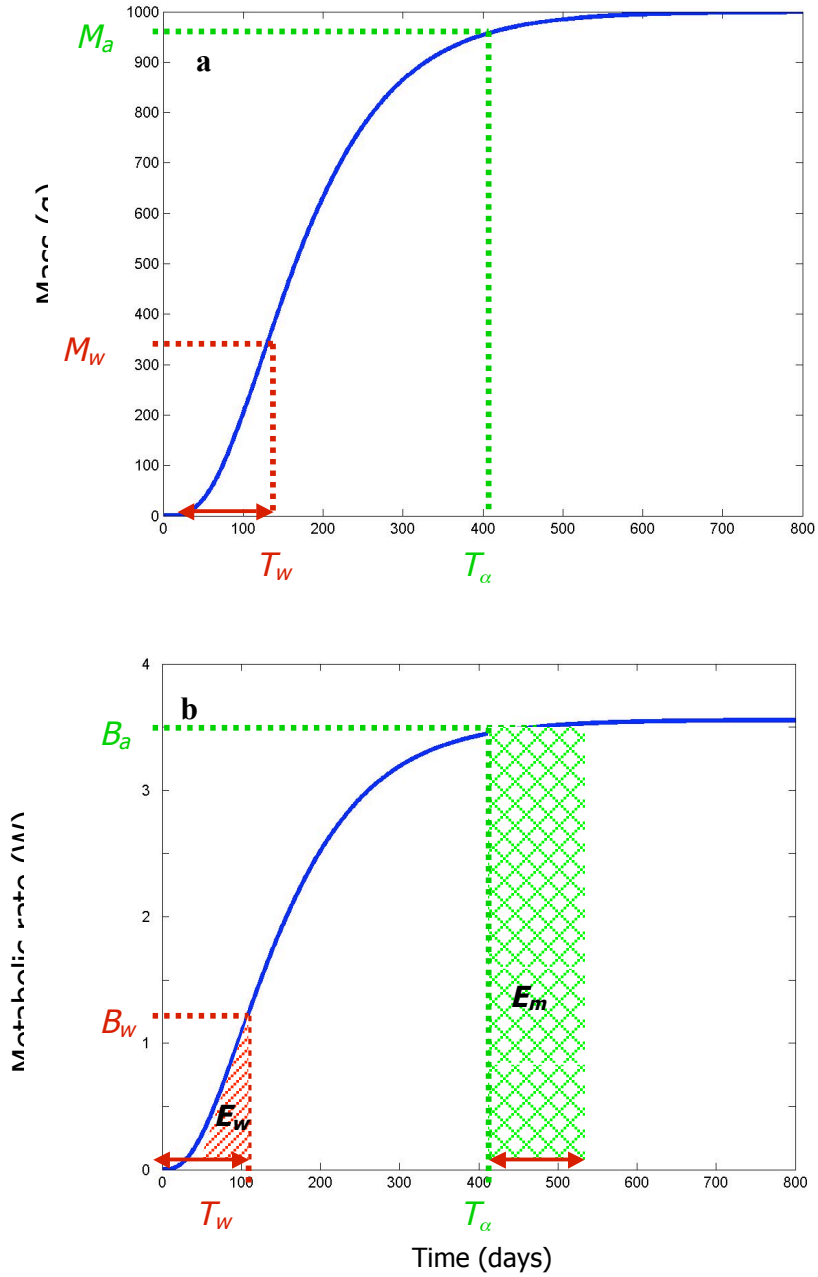

Figure 3.5 Mass and metabolism as functions of time according to the OGM. **(a)** The blue curve shows mass as a function of time. Growth occurs via the equation $dm/dt = am_t^{3/4} - b_1 m_t$ where m_t is mass at time t, and a and b_1 are constants. Adult mass (M_a) equals theoretical maximum size (M) for this hypothetical 1000 g mammal. Growth from conception to the mass at weaning ($M_w = \delta M_a$) requires time T_w and growth to M_a requires time T_α. **(*b*)** The blue curve shows metabolism as a function of time for the same hypothetical 1000g mammal. Metabolic rate (B_t) is a function of mass at time t: $B_t = B_0 m_t^{3/4}$ where B_0 is a scaling pre-factor. The energy (E_w) required to grow to size M_w is $B_0 m_t^{3/4}$ integrated over time period T_w as indicated as the red shaded area. The maternal metabolism integrated over this same time period is $B_0 M_a^{3/4} T_w$ and is represented by the green shaded area.

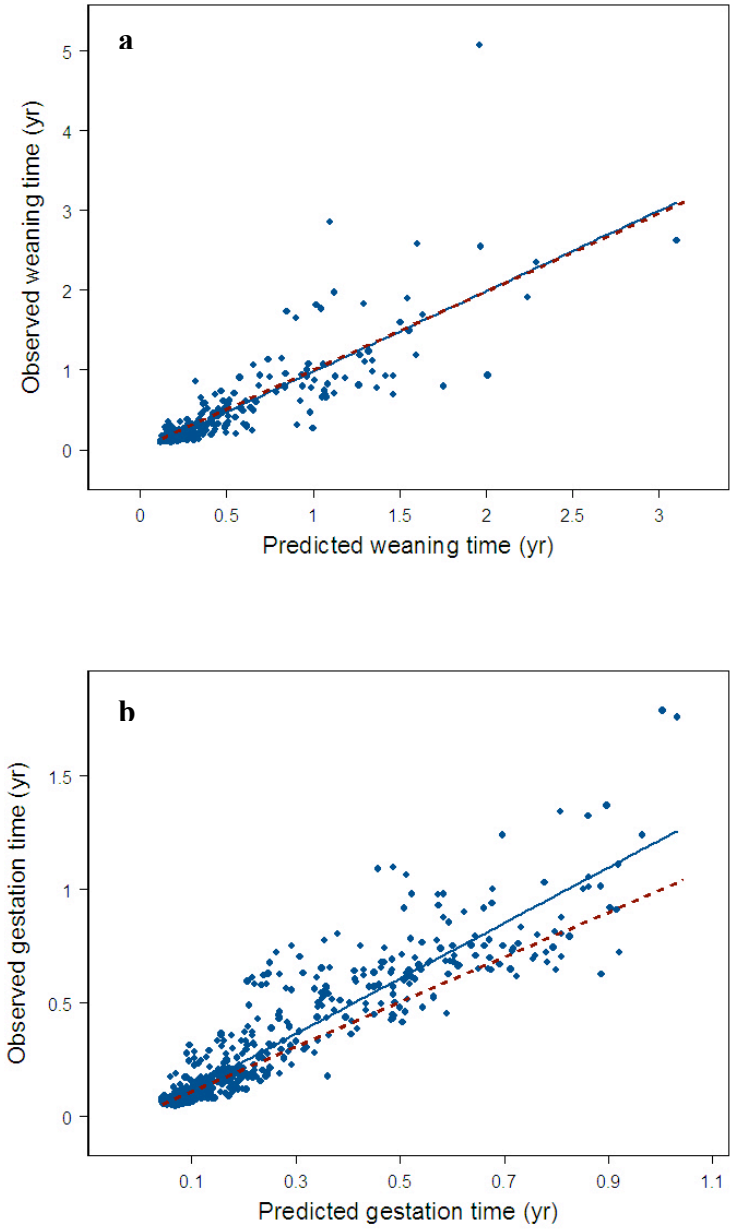

Figure 3.6 Observations versus predictions of the OGM. **(a)** Time from conception to weaning. The dashed line is the 1:1 line and the solid line is the regression line: Observed T_w = 1.01(Predicted T_w) – 0.03 (r^2 = 0.69, n = 297, p < 0.001. The 1:1 line is within the 95% CI of the regression slope). **(*b*)** Gestation time. The dashed line is the 1:1 line and the solid line is the regression line: Observed time to gestation = 1.22 Prediction – 0.003 (r^2 = 0.85, n = 602, p < 0.001).

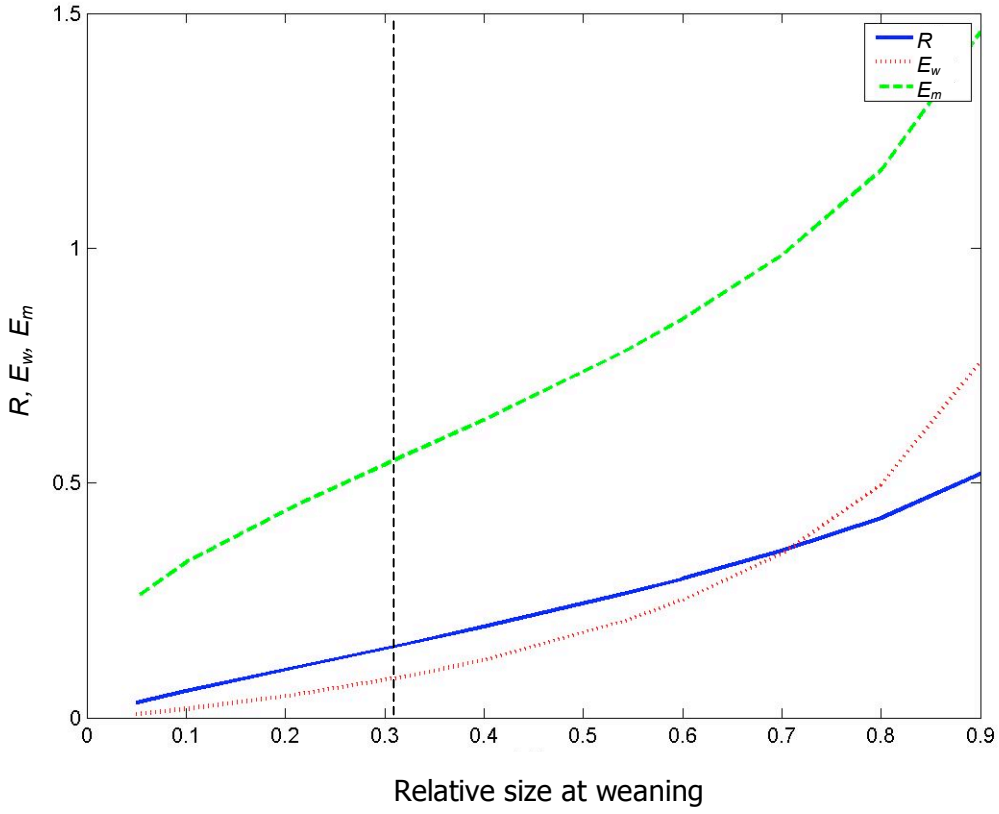

Figure 3.7 The energy for offspring to grow to the relative size at weaning (δ). The metabolic energy of the mother (E_w) integrated over the parental care period (E_m) and relative reproductive effort ($R = E_w / E_m$) are shown as functions of δ. R, E_w, and E_m are calculated at 0.1 intervals of δ. The observed value of δ is indicated by the dashed vertical line.

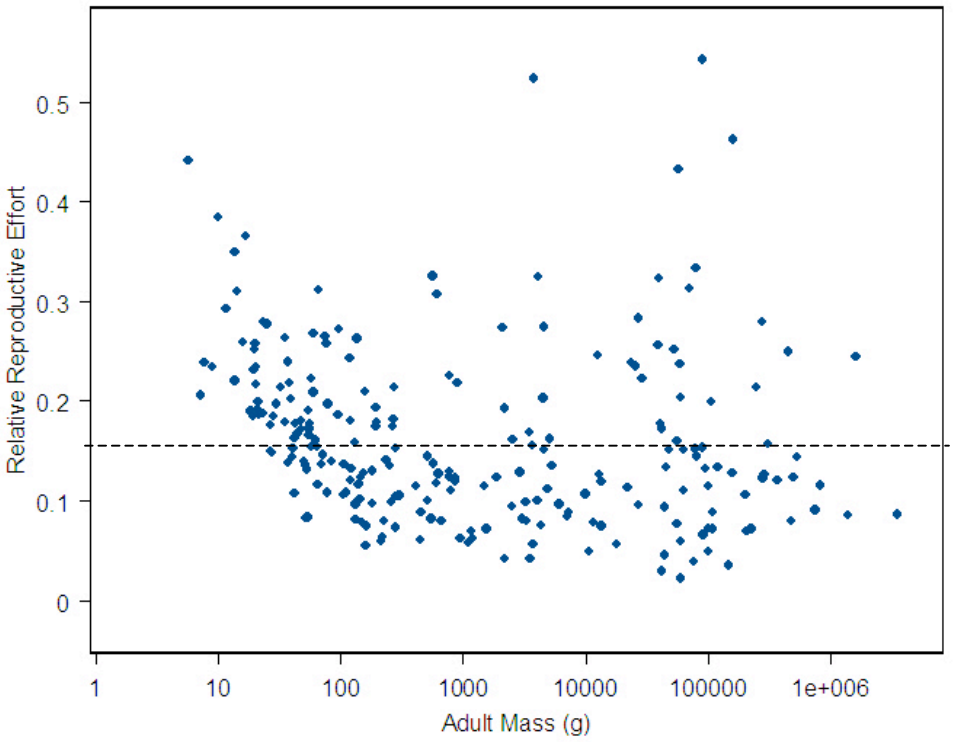

Figure 3.8 Relative reproductive effort (R) as a function of adult mass. Mean R is 0.16 and is indicated by the dashed line. Although there is substantial variation in R, R is not significantly influenced by M_a ($F = 1.07$, $n = 229$, $p = 0.301$).

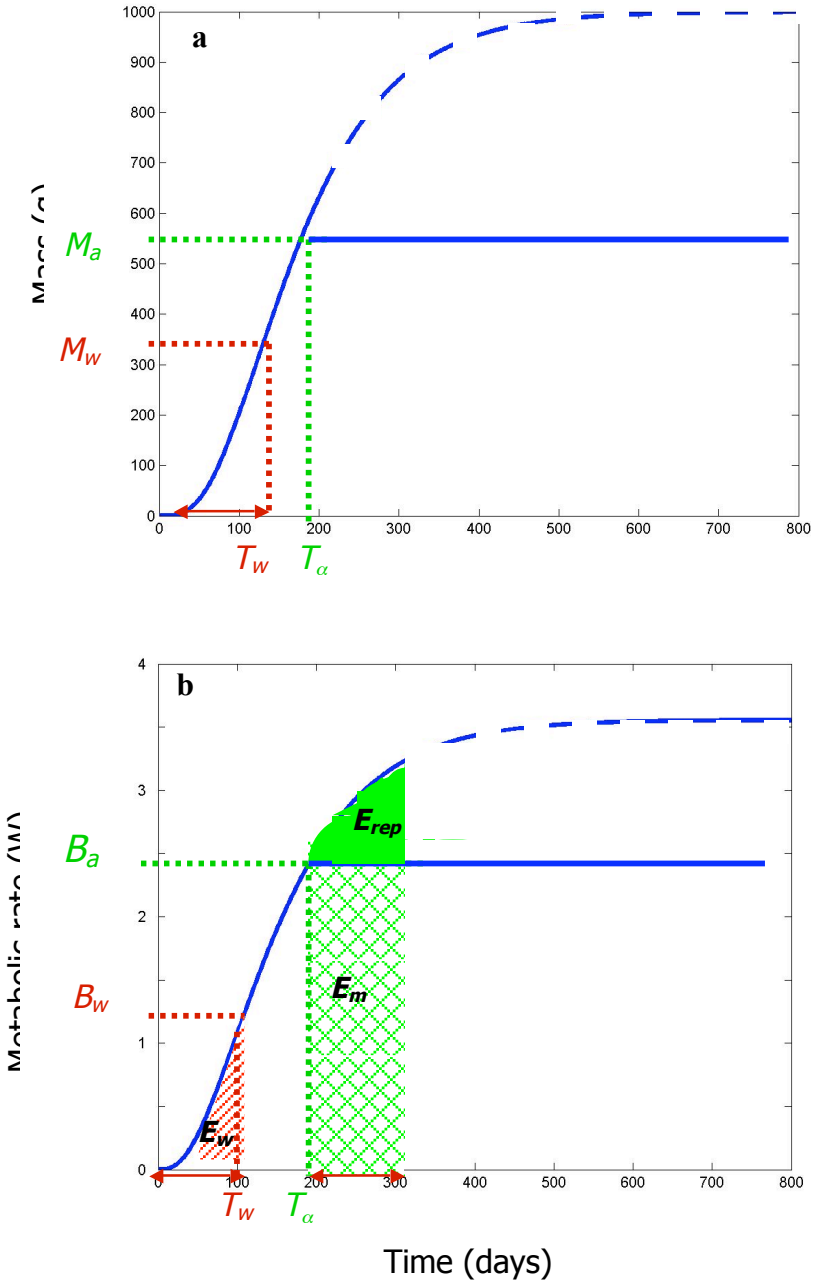

Figure 3.9 Mass and metabolism as functions of time with reproductive energy diverted from growth. **(a)** Mass as a function of time according to Charnov (2001). Growth is similar to growth in the OGM (Figure 3.5a), but growth ceases at some fraction, μ, of theoretical maximum mass, M. In this example, $\mu = 0.54$. As a result $M_a = \mu M$ as indicated by the solid blue line, and T_α is shortened. **(b)** Metabolism as a function of time when growth follows the trajectory described by Charnov (2001). E_w and E_m are the same as in Figure 3.5b. Charnov suggests that the energy available for reproduction (E_{rep}) is equal to the energy diverted from growth to the theoretical maximum mass M. In the calculations presented here, $E_{rep} = E_m$ when $\mu = 0.54$.

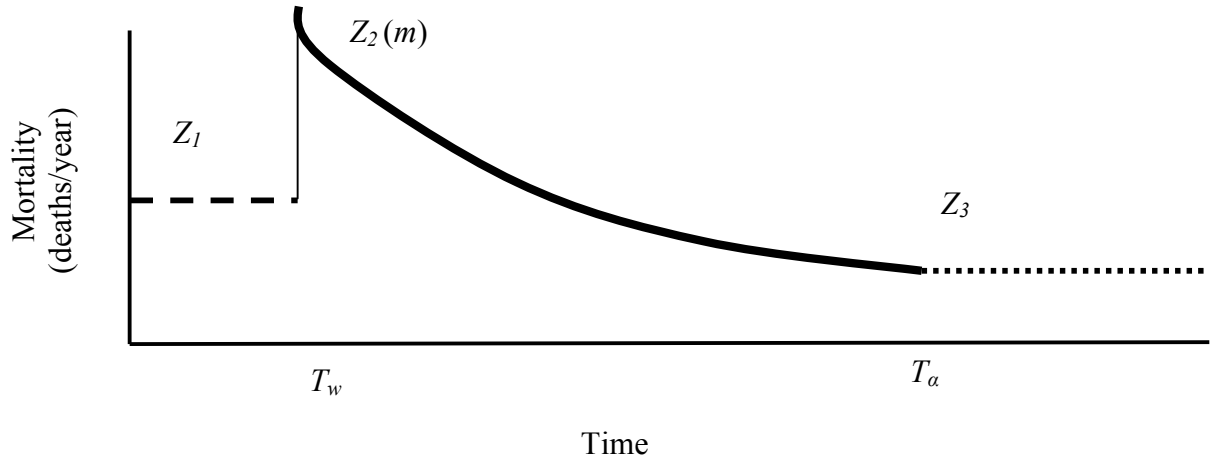

Figure 3.10 A schematic diagram of mortality rates as a function of time from birth to maturity. Z_1 is the juvenile mortality rate during the parental care period and is assumed to be constant. Z_2 is the juvenile mortality rate between weaning and adult size. Z_2 is a declining function of mass (m), therefore it declines over time as the organism grows. Z_3 is the adult mortality rate and is assumed to be constant. The figure is modified from Charnov (2001).

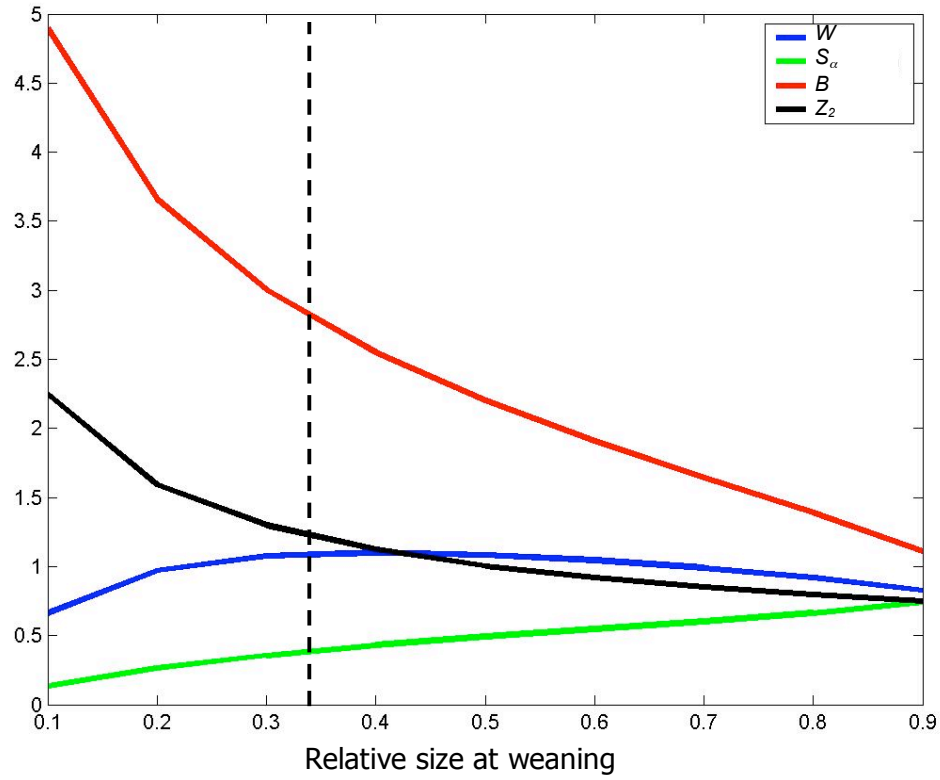

Figure 3.11 Parental fitness (W), annual birth rate (b), annual juvenile mortality rate (Z_2) and survival to maturity (S_α) as functions of relative size at weaning (δ). In this simulation, $p = 4$, $q = 0.5$, and $Z_2 = pZ_1\delta^{-q}$. These values generate S_α which is maximum near the mean value of δ from Ernest (2003), indicated by the dashed line.

4 THE EFFECT OF COLONY SIZE ON FORAGING ACTIVITY IN ANTS: THEORY AND OBSERVATIONS FROM THE GENUS *POGONOMYRMEX*

4.1 ABSTRACT

The Allometric Network Travel and Search (ANTS) model was developed to describe optimal colony foraging as a function of colony size. Field observations of *Pogonomyrmex rugosus*, *P. maricopa and P. desertorum* were conducted in New Mexico and Arizona in the summers of 2003 and 2004 to test the ANTS model. The model predicts time spent traveling from the nest to seed search locations as a function of colony size, and observations were in quantitative agreement with the model. The density of foraging ants was highest for large colonies, in qualitative agreement with the model. However, the ANTS model did not account for one apparent advantage of large colony size. Large colonies appear to minimize seed search times by foraging in areas with high seed density, including areas in the territories of smaller colonies.

Large and small colonies appear to employ different foraging strategies, each designed to minimize foraging time such that foraging times of individual ants are very similar across a 30-fold difference in colony size. These similar foraging trip times suggest that the metabolic intake rate of colonies scales isometrically with forager population size. Because large and small colonies employ these different strategies, otherwise ecologically similar colonies may be able to coexist in the same community. This chapter is coauthored by Bruce T. Milne and is currently in preparation for publication.

4.2 INTRODUCTION

Optimal foraging theory assumes that animals have evolved foraging behaviors that maximize their return on investment in terms of time and energy (Stephens & Krebs 1986). Central place foragers are constrained in that they must travel to and from a central place while acquiring resources. Central place foraging theory predicts how such foragers maximize net energy intake based on food selectivity and the cost of traveling from the nest to the food and back again (Orians & Pearson 1979).

Harvester ants have frequently been used to test optimal foraging theory, particularly central place foraging theory (Traniello 1989, Bailey & Polis 1987, Weier & Feener 1995, Fewell 1988, Morehead & Feener 1998). These studies have focused on the foraging trips of individual ants, which often fail to satisfy theoretical predictions. Morehead & Feener (1998) suggest that some foraging ants may not follow theoretical predictions because they violate the unstated assumption that all foragers behave independently of one another.

We present a foraging model that explicitly assumes that foraging ants in a colony do not behave independently of one another. Instead, we assume that foragers behave to maximize the fitness of the colony (Oster & Wilson 1978). The distribution of foragers and resources in the territory areas of harvester ant colonies affect the rate of resource acquisition of the colony (Brown & Gordon 2000) and ultimately may affect reproductive success (Gordon & Wagner 1997). We suggest that the size of a colony is an important component of its design that influences the way in which colonies acquire resources from the environment. Here we present a model that predicts how the number of foragers in a

colony affects optimal foraging behavior. We also present observations of *Pogonomyrmex* foraging activity in the Chihuahuan Desert and short grass prairie of New Mexico and compare those observations to model predictions.

4.2.1 *Colony Size*

The size of an ant colony may be measured in a number of ways: total colony biomass, territory area, nest volume, or total number of workers. Here we focus on number of workers, which ranges over eight orders of magnitude across all known ant species (Kaspari & Vargo 1995). The *Pogonomyrmex* species in this study are similar in diet, behavior, and temperature tolerance (Johnson 2000), but their asymptotic colony sizes range from 400 to 10,000 workers per colony (Table 4.1). Asymptotic colony size is reached after several years, after which time average colony size remains relatively constant despite annual and seasonal fluctuations (Gordon 1995a, Johnson 2000).

Number of workers is an ecologically important attribute of a colony. It affects competitive ability (Holway & Case 2001), the latitudinal distribution of species (Kaspari & Vargo 1995), territory area (Gordon 1995a) and foraging strategy (Beckers *et al.* 1989, Oster & Wilson 1978, Davidson 1977).

Number of foragers is a useful index of colony population size. The foragers retrieve food from the environment to supply the metabolic needs of the colony. The rate at which a colony acquires resources can be estimated from the number of foragers and the average rate at which each forager retrieves food.

4.2.2 *An Allometric Understanding of Ant Foraging Networks*

Allometry provides a theoretical explanation for the ecologically important relationships between organism size and biological rates (Brown *et al.* 2004). Allometric theory posits that the properties of metabolic networks scale non-linearly with body size, resulting in biological rates that also scale non-linearly with body size.

Allometric theory is relevant to the study of ant foraging behavior. Colony size has a nonlinear effect on territory area in *Solenopsis invicta* (Tschinkel *et al.* 1995) and on nest volume, colony growth rate and seed collection efficiency in *Pogonomyrmex badius* (Tschinkel 1999). Patterns of foraging activity constitute networks that function to distribute information (Adler & Gordon 1992), explore territory (Gordon 1995b), establish foraging ranges (Adler & Gordon 2003), recruit workers and retrieve resources (Beckers *et al.* 1989). Some of these networks are virtual, or at least ephemeral and poorly defined, although many trunk-trail foragers, including *P. rugosus,* may forage in densely packed, highly organized columns which leave physical trails in the landscape.

Jun *et al.* (2003) proposed an allometric ant foraging model which hypothesized that fractal foraging trails cause foraging times to be a nonlinear function of forager population size. Here we do not specify the geometry of foraging trail networks; rather, we investigate the effect of the size of a foraging network (measured by the number of foragers) on foraging times and the distribution of foragers in the territory area.

4.3 DESCRIPTION OF THE ANTS MODEL

The Allometric Network Travel and Search (ANTS) model examines how the size of a network of foragers affects optimal foraging behavior and rates of resource acquisition. The model predicts that foraging distances and times will be non-linear functions of forager number.

The model describes foraging by stationary colonies that consume stationary resources. It compares colonies that differ fundamentally only in forager numbers and the distribution of those foragers in the colony territory. It assumes the foragers are identical in their abilities to search for, choose and transport seeds, and all colonies are assumed to consume energetically equivalent food. The model is based on observations of *Pogonomyrmex* foragers that maximize energy gain by minimizing the foraging time of individual ants (Fewell 1988, Morehead & Feener 1998, Weier & Feener 1995). Since *Pogonomyrmex* foragers begin a new foraging trip immediately after delivering a seed to the nest, seed intake rate is proportional to the number of foragers divided by the average time of a foraging trip. Thus, for a given number of foragers, minimizing foraging trip time maximizes the metabolic intake rate of the colony.

The goal is to determine how a colony can minimize the average time of a foraging trip (T_f) given a number of foragers (F). The time to complete a foraging trip can be divided into 1) time to complete outbound travel to a search location, 2) time to search a patch, and 3) time of inbound travel back to the nest (Traniello 1989, Weier & Feener 1995). Here, travel time (T_t) is the average time a forager spends traveling to and

from a search location. Generally, a traveling forager moves rapidly in a relatively straight path.

The average time spent actively searching for seeds is T_s. Searching is characterized by slower, diffusive movement and frequent stops to examine patches of grass or depressions in soil which are likely to harbor seeds. Both T_t and T_s are mean values for all foragers in a colony; the average duration of a foraging trip is the sum of T_t and T_s.

$$T_f = T_s + T_t \qquad [4.1]$$

The ANTS model assumes that individual ants forage according to Equation 4.1 with T_t and T_s defined as functions of F.

T_t is determined by the way ants fill the space of their foraging territory. If the foragers were distributed in their respective colony territories with equal density in all colony sizes, the size of a foraging area would be a linear function of forager population size (F). Then both the maximum and average distances that a forager must travel to acquire resources would increase with the square root of colony size. Assuming equivalent travel speeds across colonies, then $T_t \sim F^{1/2}$. Since T_t represents the per ant travel time, the total time all ants in a colony spend traveling is proportional to $T_t F$ which is proportional to $F^{3/2}$. Thus, increasing colony size results in individual ants spending more time traveling, or, viewed from the perspective of the colony, the total amount of travel time increases faster than colony size increases.

The ANTS model posits that larger colonies can reduce T_t if they utilize a higher density of foragers (ρ_f) in their territories. Higher ρ_f reduces the size of the territory area (A) and thereby reduces travel distances and T_t.

However, increasing ρ_f also bears a foraging time cost. In the model, T_s is inversely related to seed density (ρ_s) because when there are fewer seeds, it takes foragers longer to find them. As ρ_f increases, seeds are depleted faster, and as ρ_s decreases, T_s increases. Larger colonies then face a tradeoff between larger territories (with relatively long T_t and short T_s) or higher density of foragers in smaller territories (with relatively shorter T_t and longer T_s). The ANTS model calculates the optimal forager density (ρ_f*) that minimizes T_f and describes how ρ_f* changes as a function of colony size.

4.4 Summary of the ANTS Model Predictions

The quantitative predictions of the ANTS model include travel distance, travel times, search times, forager density and total foraging trip times (Table 4.2). The derivation of these predictions appears in the Appendix in Section 4.9. In summary, the ANTS model predicts that larger colonies will have larger territories and will have a higher density of foragers in the territory. The foragers in large colonies will travel further to search for food and will have longer travel times. As long as seed density and the speed and search efficiency of individual foragers are constant, the model predicts that foragers in large colonies will also have longer search times, and therefore the total length of foraging trips will be longer.

4.5 METHODS

The ANTS model variables and the methods by which each variable was measured in the field are listed in Table 4.1. In the summer of 2003, preliminary observations were made on 8 colonies of *P. desertorum, P. maricopa,* and *P. rugosus* on the Sevilleta Long Term Ecological Research Site in New Mexico and in Portal, Arizona. In 2004, the study employed a nested design of 4 colonies each of *P. desertorum, P. maricopa* and *P. rugosus,* all on the Sevilleta. Thus, a total of 20 colonies were observed over the 2 years. 154 completed foraging trips were observed and there were sufficient data to estimate the model variables for 16 colonies.

Each of the three species has a different characteristic number of workers and foragers (Table 4.1). Although the number of foragers active during any foraging period is somewhat plastic, the asymptotic colony size differs consistently among species (Johnson 2000). The three focal species are sufficiently different in colony size that daily fluctuations in foraging activity should not mask general trends in forager number.

The following observations were made for each colony under natural field conditions. Individual foragers were followed as they left the nest, traveled to a search location, searched for and acquired a seed, and returned to the nest. Some foragers were marked with DecoColor opaque paint markers ® Uchida of America. Others were left unmarked and were followed with careful observation. For each forager, T_f, T_s, T_t, d_t, and v_t were measured by methods in Table 4.1. The entrance(s) to each colony were monitored to estimate F for each colony. Temperature at 2 cm above ground was recorded with a thermocouple.

Additional observations and experimental manipulations were made for the 12 colonies observed in 2004. To test the effect of seed density on search times, six 1 m^2 quadrats were

established in each colony territory for seed addition experiments. Three quadrats were placed randomly at each of 2 distances from the nest entrance (at 3 m and 6 m from *P. desertorum* nest entrances, and at 6 m and 12 m from *P. maricopa* and *P. rugosus* nest entrances; Figure 4.1). The quadrats were observed for 300 s intervals. In each interval we recorded: number of seeds removed, time spent searching for each found seed, and whether each forager was searching or traveling. We also recorded the number of searchers and travelers at the start and end of each interval. For each colony, observations of the quadrats were made on two days under control conditions. On two additional days, 150 millet seeds were added to two of the 1 m^2 plots and the same measurements were made.

4.6 RESULTS

4.6.1 *Allometric Scaling Patterns*

Travel distance (d_t), travel time (T_t), search time (T_s), foraging time (T_f), forager density (ρ_f), territory area (A) and the number of foragers (F) were measured for each colony (Table 4.1). The ANTS model predicts that d_t, T_t, ρ_f, A, T_s and T_f all increase non-linearly with F. In the colonies observed, d_t, T_t, ρ_f, and A, increase significantly with F, but T_s and T_f do not (Figure 4.2).

Some variables are significantly different among species. d_t and T_t in *P. desertorum* differed significantly from *P. maricopa* and *P. rugosus* (Table 4.2). F, ρ_f and A in *P. rugosus* differed significantly from *P. desertorum* and *P. maricopa.* T_s and T_f did not differ significantly between species. None of the parameters varied significantly

between years without controlling for species effects, but there was a significant difference between years in *P. desertorum* for T_s ($F = 8.40$, $n = 48$, $p = 0.0057$) and T_f ($F = 11.45$, $n = 48$, $p = 0.0015$).

4.6.2 *Travel Distance and Travel Time*

Equations 4.2 and 4.3 predict that d_t and T_t increase with colony size and decrease with forager density. v_t averaged 0.036 m/s and was indistinguishable across species ($F = 2.89$, $n = 114$, $p = 0.06$) although *P. rugosus* were slightly faster than the other species. The observed d_t and T_t are indistinguishable from the model predictions for each species (Figure 4.3).

The travel time prediction is based on the assumption that the density of searching foragers does not vary with distance from the nest. This was tested by measuring the density of actively searching foragers at grids placed at 2 distances from the nest entrance. Figure 4.4 shows that the density at the two distances was indistinguishable in all 3 species.

4.6.3 *Search Time*

The ANTS model predicts that T_s decreases as ρ_s increases (Equation 4.4). Field observations provide qualitative support for this prediction. T_s was shortest in quadrats that were supplemented with seeds (Figure 4.5a).

Since the density of foragers (ρ_f) is expected to decrease the density of seeds (ρ_s), T_s is expected to increase as ρ_f increases. Quantitative comparisons between observed search times and model predictions require knowing the efficiency of seed detection (E_s), the diffusion rate of searching foragers (D_s), and the density of seeds (ρ_s). Reliable measurements of E_s, D_s, and ρ_s were not obtained. If they are assumed to be equivalent across species, the model predicts that T_s is an increasing function of ρ_f. However, there was no significant relationship between T_s and ρ_f in the observations (Figure 4.5b). Additionally, there was no increase in T_s with time of day ($F = 0.084$, $n = 119$, $p = 0.77$), implying that forager depletion of seeds did not increase the search times of subsequent foragers.

4.6.4 *Optimal Forager Density*

We expect forager density in the field to approximate ρ_f^* since colonies with this density of foragers should minimize T_f. ρ_f^* is predicted to increase as a function of F and decrease as a function of T_s (Equation 4.8). ρ_f^* increased significantly as a function of F (Figure 4.2c), but showed no significant relationship to T_s (Figure 4.5b). A quantitative comparison between the model prediction and the observations is not possible because E_s and D_s were not measured in the field.

4.6.5 *Foraging Times*

The model predicts that if search efficiency and seed density are equal across colonies, both T_t and T_s will be longer in larger colonies, thus T_f will also be longer in larger colonies. However, T_f was indistinguishable across species (Table 4.3).

T_f was also indistinguishable between years without considering an interaction with species effect; however, mean T_f for *P. desertorum* is almost twice as long in 2003 than in 2004 (Figure 4.6) and the difference was significant ($F = 11.45$, $n = 48$, $p = 0.0015$).

4.6.6 *Recruitment and Invasion*

Each species showed a different pattern of recruitment to dense seed patches (Figure 4.7a). *P. desertorum* doubled the searchers per quadrat per observation period when seeds were added; however, the increase may not have been caused by recruitment. *P. desertorum* never exploited seeds added to the far quadrats, and in the closer quadrats (3m from the nest), the increase in searcher density appeared to be created by the same individuals rapidly returning to the foraging site, so that the same forager was often counted twice within the 300 s period. Thus, the apparent increase in searcher density was largely due to the close proximity of the quadrat to the nest.

P. maricopa appeared not to recruit additional workers to the near quadrat, and like *P. desertorum,* never exploited seeds in the far quadrat. *P. rugosus* was the only

species that appeared to recruit workers to both near and far sites. On average, *P. rugosus* tripled the number of searching foragers in seed addition plots.

P. maricopa and *P. rugosus* each retrieved seeds from seed addition plots located in the foraging areas of smaller species. *P. desertorum* did not exploit seeds in any other species' territories (Figure 4.7b).

4.7 DISCUSSION

Pogonomyrmex colonies adjust their foraging behavior based on forager population size (Table 4.1, Figure 4.2). Without invoking the specific geometry of foraging networks, the allometric approach suggests that there is a non-linear relationship between the distance to seeds and the size of the network of foraging ants. In quantitative agreement with the ANTS model predictions, large colonies send their foragers further distances to collect seeds and therefore foraging travel times are longer (Figures 4.2a, 4.2b and 4.3). The model also predicts that large colonies distribute their foragers in the territory with higher density than do smaller colonies, and this was also observed (Figure 4.2c).

The ANTS model predicts that foragers in larger colonies have longer search times, but there was no significant increase in search time with colony size (Figures 4.2e and 4.5a). Colonies with higher forager density may not have had increased search times (Figure 4.5b) because those colonies were able to recruit workers to patches with high seed density (Figure 4.7). As a result, total forager trip times were invariant with respect to forager number (Figures 4.2f and 4.6). Since the rate at which a forager returns seeds to the nest is the inverse of foraging trip time, seed intake rate per forager is invariant

with respect to the number of foragers in the colony. Thus, in the species studied here, colony metabolic intake scales isometrically with colony size.

In eusocial colonies, the foraging activity of one forager can affect the foraging success of another. Regardless of whether colonies use individual foraging strategies (as in *P. desertorum*) or group foraging strategies and trunk trails (as in *P. rugosus*), foragers travel from a central location to gather food in the same territory. Food acquired by one forager becomes unavailable to the other foragers. In larger colonies with larger territories, some foragers have to go greater distances to acquire seeds to avoid competition for limited seeds close to the nest.

Central place foraging theory predicts that individual foragers that travel further will be more selective in choosing seeds, but this has not been observed in field studies (Bailey & Polis 1987, Fewell 1988, Morehead & Feener 1998). It is possible that this deviation from theory occurs because some foragers must travel greater distances not to forage optimally as individuals, but to forage optimally for the colony.

Species of ecologically similar *Pogonomyrmex* seed harvesters often coexist when the species have very different colony sizes (Johnson 2000). Body size can mediate resource partitioning in ants (Davidson 1977, Chew & DeVita 1980). This study suggests that colony size may also affect resource partitioning. Even though there is significant dietary overlap in the species of seeds these ants consume (Davidson 1977, Johnson 2000), these ants may divide niche space in a way that enables coexistence because each species forages in a way that is optimal for its colony size. Species with smaller colonies appear to forage for sparsely distributed seeds, while the larger colonies exploit dense seed patches (Figure 4.7).

Large colonies obviously consume more resources than small colonies. Additionally, field observations suggest that larger colonies collect more resources per unit area. Large colonies have more foragers per unit area, with each forager removing resources at approximately the same rate (Figure 4.2c and 4.2f). The rate at which seeds are consumed per unit area may affect the interactions that ants have with plants and other granivores.

Field observations showed no relationship between search time and forager density. The ANTS model predicts that search times increase with forager density, but only if seed density does not vary as a function of colony size. Observations would be reconciled with model predictions if large colonies foraged in areas with higher seed densities. Larger colonies may be located in regions with higher seed density, or they may exploit dense seed patches at a smaller scale.

The species on the Sevilleta are interspersed, but not all species occur in all plots. One region of the Sevilleta contains only *P. rugosus,* while other regions contain all three species. This might suggest that *P. rugosus* dominates areas with higher seed density, thus lowering search times. However, there is not a significant relationship between colony location and search time within *P. rugosus* ($F = 0.835$, $n = 40$, $p = 0.457$).

Alternatively, larger colonies may be better able to recruit to dense seed patches, to invade the core foraging areas of smaller colonies, and perhaps to defend their own core areas from incursions from smaller colonies (Figure 4.7). Thus, although large colonies may be intermingled with smaller colonies in the landscape, they may be able to concentrate their foragers in patches with higher seed density. By increasing forager

density and recruitment to high quality patches, large colonies maintain per ant foraging times (and therefore per ant food intake rates) equivalent to small colonies.

The ANTS model postulates that colonies should be selected to minimize foraging times, but there are many factors other than colony size that affect foraging behavior and energy intake rates, and many of those factors may be correlated with colony size. For example larger colonies tend to utilize recruitment, chemical communication networks and trunk trails more frequently (Holldobler 1976, Beckers *et al.* 1989, Anderson & McShea 2001). Additionally, colonies may differ in length of daily or seasonal foraging period, efficiency of energy extraction from seeds, or ability to select higher quality seeds. Integrating forager population size with other components of optimal foraging theory may provide a better understanding of how ants, and perhaps other social organisms, optimize energy acquisition.

The largest *P. rugosus* colony (2300 foragers) had 30 times more foragers and a territory 10 times larger than the smallest *P. desertorum* colony (65 foragers). However, with a 4-fold increase in forager density, *P. rugosus* colonies only had to send their foragers twice as far as *P. desertorum* colonies. This small increase in travel distance and time was compensated for with small decreases in search time.

Thus, across a large difference in forager number, all colonies had similar mean foraging trip times within each year of the study. Since foraging trip time was invariant with respect to colony size, metabolic intake rates scale isometrically with forager population size. This is in contrast to metabolism that scales allometrically with body size in individual organisms.

The ANTS model makes explicit the foraging costs and benefits associated with increased colony size. Colonies pay a foraging cost in that individuals must travel further to acquire resources, but there is also a foraging benefit. Large colonies appear to use their foraging network to gain information about the location of rich resource patches and they exploit that information to allow a higher density of foragers in the landscape without increasing search times. The tradeoff between a geometric cost and a benefit of exploiting information may have implications for other social organisms.

4.8 REFERENCES

Adler, F. R. & Gordon, D. M. (1992). Information collection and spread by networks of patrolling ants. *Am. Nat.*, **140**, 373–400.

Adler, F.R. & Gordon, D.M. (2003). Optimization, conflict and non-overlapping foraging in ants. *Am Nat,* **162**, 529-543.

Anderson, C. & McShea, D. W. (2001). Individual versus social complexity, with particular reference to ant colonies. *Biol. Rev.,* **76**, 211–237.

Bailey K.H. & Polis, G.A. (1987). Optimal and central-place foraging theory applied to a desert harvester ant, *Pogonomyrmex californicus*. *Oecologia,* **72**, 440-448.

Beckers, R., Goss, S., Deneubourd, J.L. & Pasteels, J.M. (1989). Colony size, communication and ant foraging strategy. *Psyche,* **96**, 239-256.

Brown, J.H., Gillooly, J.F., Allen, A.P., Savage, V.M. & West, G.B. (2004). Toward a metabolic theory of ecology. *Ecology,* **85**, 1771-1789.

Brown, M.J.F. & Gordon, D.M. (2000). How resources and encounters affect the distribution of foraging activity in a seed-harvesting ant. *Behav. Ecol. Sociobiol.,* **47**, 195-203.

Chew, R. M. & DeVita, J. (1980). Foraging characteristics of a desert ant assemblage: functional morphology and species separation. *J. Arid Environ.*, **3**, 75-83.

Davidson, D.W. (1977). Foraging ecology and community organization in desert seed eating ants. *Ecology,* **58,** 725-737.

Fewell, J.H. (1988). Energetic and time costs of foraging in harvester ants, *Pogonomyrmex occidentalis. Behav. Ecol. Sociobiol.,* **22**, 401-408.

Gordon, D.M. (1984). Species-specific patterns in the social activities of harvester ant colonies (*Pogonomyrmex*). *Insect. Soc.,* **31**, 74-86.

Gordon, D.M. (1995a). The development of an ant colony's foraging range. *Anim. Behav.,* **49**, 649-659.

Gordon, D.M. (1995b). The expandable network of ant exploration. *Anim. Behav.,* **50**, 995-107.

Gordon, D. M., & Wagner, D. (1997). Neighborhood density and reproductive potential in harvester ants. *Oecologia*, **109**, 556–560.

Holldobler, B. (1976). Recruitment behavior, home range orientation and territoriality in harvester ants, *Pogonomyrmex*. *Behav. Ecol. Sociobiol.,* **1**, 3-44.

Holldobler, B. & Wilson, E.O. (1990). *The Ants.* Harvard University Press, Cambridge, MA.

Holway, D.A. & Case, T.J. (2001). Effects of colony-level variation on competitive ability in the invasive Argentine ant. *Anim. Behav.*, **61**, 1181-1192.

Johnson, R.A. (2000). Seed-harvester ants (*Hymenoptera formicidea*) of North America: An overview of ecology and biogeography. *Sociobiology,* **36**, 83-122.

Jun, J., Pepper, J.W., Savage, V.M., Gillooly, J.F. & Brown, J.H. (2003). Allometric scaling of ant foraging trail networks. *Evol. Ecol. Res.,* **5**, 297-303.

Kaspari, M. & Vargo, E.L. (1995). Colony size as a buffer against seasonality: Bergmann's rule in social insects. *Am. Nat.*, **145**, 610-618.

Mackay, W.P, MacKay, E. & Song, W. (2002). *Ants of New Mexico.* Edwin Mellen Press.

Morehead, S.A. & Feener, D.H. (1998). Foraging behavior and morphology: Seed selection in the harvester ant genus, *Pogonomyrmex*. *Oecologia***, 114**, 548-555.

Orians, G.H. & Pearson, N.E. (1979). On the theory of central place foraging. In *Analysis of Ecological Systems*. (eds. Horn, D.J., Stairs, G.R., & Mitchell, R.D.). Ohio State Univ. Press, Columbus, 155-177.

Oster, G.F. & Wilson, E.O. (1978). *Caste and Ecology in the Social Insects.* Princeton University Press, Princeton.

Stephens, D.W. & Krebs, J.R. (1986). *Foraging Theory.* Princeton University Press, Princeton.

Traniello, J.F. (1989). Foraging strategies of ants. *Annu. Rev. Entomol.,* **34**, 191-210.

Tschinkel, W.R., Adams, E.S. & Macom, T. (1995). Territory area and colony size in the fire ant *Solenopsis invicta. J. of Anim. Ecol.,* **64**, 473-480.

Tschinkel, W.R. (1999). Sociometry and sociogenesis of colony-level attributes of the Florida harvester ant (*Hymenoptera formicidae*). *Ann. Entomol. Soc. Am*.,**92**, 80-89.

Weier, J.A. & Feener, D.H. (1995). Foraging in the seed-harvester ant genus *Pogonomyrmex*: Are energy costs important? *Behav. Ecol. Sociobiol.,* **36**, 291-300.

4.9 APPENDIX: DERIVATION OF THE ANTS MODEL

4.9.1 *Derivation of Travel Time*

Travel time (T_t) is the distance traveled to a seed (d_t), divided by the travel velocity (v_t), and multiplied by 2 to account for the return to the nest: $T_t = 2d_t v_t^{-1}$. v_t is assumed to be constant with respect to F, but d_t depends on the size of the colony territory and the way in which foragers are distributed in that territory. T_t is computed as the average travel time of all foragers in a colony.

Several assumptions are made to simplify the problem. The territory area (A) of each colony is assumed to be circular, and interactions from neighboring colonies are not considered. We define density of foragers (ρ_f) as the average number of foragers actively searching in each m^2 of territory area. (Note that there will be other foragers traveling in the territory, but ρ_f refers only to foragers who are searching). The foraging area of a colony is determined by the number of foragers and the density with which those foragers search the territory: $A = F/\rho_f$.

The maximum distance any forager can travel (d_{tmax}) is the radius of the colony territory area, so that $d_{tmax} = (A/\pi)^{1/2} = F^{1/2}(\rho_f \pi)^{-1/2}$. Many foragers will have searched locations closer to the nest, thus they will have traveled less than d_{tmax}. d_t is the mean distance traveled by all foragers and equal to the total distance traveled by all of the foragers ($d_{t\text{-}total}$) divided by F.

$d_{t\text{-}total}$ is found by integrating across all distances from the nest within A. The model assumes that the density of searchers shows no consistent variation with the distance

from the colony entrance. Under these assumptions, the average distance traveled by a forager can be found by calculating the number of foragers at each distance from the nest. The area of a small ring of width δd_r at distance d_r from the center is:

$A_r = \pi(d_r + \frac{1}{2}\,\delta d_r)^2 - \pi(d_r - \frac{1}{2}\delta d_r)^2 = 2\pi d_r\,\delta d_r$.

The number of foragers in area A_r is $F_r = \rho_f A_r = 2\pi\,\rho_f\,d_r\,\delta d_r$. Each of those foragers has traveled distance d_r, so $d_{t\text{-}total}$ is the integration of $F_r\,d_r$ from 0 to d_{tmax}:

$d_{t\text{-}total} = \int_0^{d_{tmax}} (2\pi\,\rho_f\,d_r^2\,\delta d_r)$. Solving the integral gives

$d_{t\text{-}total} = 2/3\pi\,\rho_f\,d_r^3\Big|_0^{d_{tmax}}$ and substituting $d_{tmax} = F^{1/2}(\rho_f\,\pi)^{-1/2}$ gives

$d_{t\text{-}total} = 2/3\pi^{-1/2}\,F^{3/2}\rho_f^{-1/2}$.

The mean distance traveled by each forager is: $d_t = d_{t\text{-}total}/F$. Calculating that $2/3\pi^{-1/2} \approx 0.38$:

$$d_t = 0.38F^{1/2}\rho_f^{-1/2} \qquad [4.2]$$

Substituting this value of d_t into $T_t = 2d_t v_t^{-1}$:

$$T_t = 0.76v_t^{-1}\,F^{1/2}\rho_f^{-1/2} \qquad [4.3]$$

4.9.2 *Derivation of Search Time*

The derivation of search time is based on the encounter rate of seeds (Stephens & Krebs 1986). T_s can be defined as a function of seed density (ρ_s), density of searchers (ρ_f), and the rate at which foragers search the territory (defined by a diffusion parameter, D_s). Search

efficiency (E_s) is the probability that a forager will find and pick up an existing seed within an area that has been searched.

Before deriving the final equation for T_s, we consider two simpler cases. First, we consider the simplest case in which foragers do not interfere with each other. If ρ_s is defined in units of seeds/m^2, then $E_s\rho_s$ is the number of seeds a forager picks up in each m^2. Then, the average number of m^2 in which the forager must search in order to find one seed is $(E_s\rho_s)^{-1}$. If the forager diffuses through the territory at rate D_s (with units m^2/s), then the time it takes to reach a new m^2 in which to search is D_s^{-1}. Thus, average search time is inversely proportional to search velocity, seed density, and search efficiency:

$$T_s = (E_s D_s \rho_s)^{-1} \qquad [4.4]$$

Equation 4.4 describes foraging times if there is no interference between foragers as they search for seeds. However, when a forager collects a seed, that seed is removed from the pool of seeds which can be collected by the other foragers. T_s then depends on the spatial and temporal scale at which foragers overlap.

Now we consider a second case in which foragers overlap in space during the search time. We assume that the foragers overlap spatially on the scale at which ρ_f and ρ_s are measured (1 m^{-2}), so that increasing ρ_f by 1 decreases ρ_s by 1 in each m^2 during that search time. Then ρ_s (in a given m^2) is diminished only by the number of foragers searching in that m^2 (ρ_f) during that search time. For the first forager to find a seed, $T_{s1} = (E_s D_s \rho_s)^{-1}$. For the second forager, $T_{s2} = [E_s D_s (\rho_s\text{-}1)]^{-1}$; for the third forager,

$T_{s3} = [\, E_s D_s (\rho_s\text{-}2)]^{-1}$; and search time increases in this way for all ρ_f foragers . The mean T_s across all of the foragers is the integral of the search time of each forager (T_{sx}) divided by the total number of foragers (ρ_f):

$$T_s = \frac{1}{E_s D_s \rho_f^{-1} \int_0^{x=\rho_f} \rho_s - x \, dx} = \frac{\rho_f}{E_s D_s (\rho_f \rho_s - \tfrac{1}{2}\rho_f^2)} \text{ so}$$

$$T_s = E_s D_s (\rho_s - \tfrac{1}{2}\rho_f)^{-1} \qquad [4.5]$$

Finally, the model considers the way in which foragers overlap through time. To simplify the consideration of temporal overlap, the model assumes that ρ_s is not altered by external factors (no seeds are added or removed, except by the ants) during the daily foraging period of the colony. In order to calculate the number of seeds removed by all foragers over a specified time period, we need to know the rate at which new foragers arrive in that m^2 (R). Assuming a steady state distribution of foragers, then newly arriving foragers are all returning foragers who have already retrieved a seed, returned to the nest and then returned to the search area. *Pogonomyrmex* foragers spend little or no time in the nest before beginning another trip (M. Moses *pers. obs.*), so the rate of return trips is $1/T_f$. Thus, $R = (T_w/T_f)$ where T_w represents the foraging period under consideration (in the *Pogonomyrmex* studied here, a foraging bout lasts about 3 hours, so $T_w = 10800$ s). Thus, the total number of foragers per m^2 per foraging period equals $R\rho_f$.

The final expression for search time, averaged over all foragers in a single day and considering the spatial and temporal overlap of foragers, is found by substituting $R\rho_f$ for ρ_f in Equation 4.5:

$$T_s = E_s D_s (\rho_s - \tfrac{1}{2} R\rho_f)^{-1} \qquad [4.6]$$

Thus, Equation 4.4 describes the search time of an individual ant searching in an area with known ρ_s. Equation 4.5 describes mean search time (T_s) when ρ_s is known at a given moment in time. Equation 4.6 describes search times when ρ_s is known at the beginning of a foraging period, and foragers deplete ρ_s over time.

According to Equation 4.6, T_s increases as the difference between ρ_s and $R\rho_f$ decreases. Simulations of Equation 4.6 are shown in Figure 4.8. In Figure 4.8a, the 360th forager to reach a patch spends nearly 10 times longer searching than the first forager to reach that patch. However, mean search time (T_s) only doubles as $R\rho_f$ approaches ρ_s. Note that $R\rho_f$ is constrained to be less than ρ_s to avoid infinite search times.

4.9.3 *Optimizing Search Strategy*

The final equation for foraging time, averaged over each forager in a colony, is obtained by substituting Equations 4.3 and 4.6 into Equation 4.1.

$$T_f = 0.76 v_t^{-1} F^{1/2} \rho_f^{-1/2} + [E_s D_s (\rho_s - \tfrac{1}{2} R\rho_f)]^{-1} \qquad [4.7]$$

The ANTS model predicts that travel time (T_t) decreases in proportion to $\rho_f^{-1/2}$, but search time (T_s) increases as a function of ρ_f. This tradeoff leads to an optimal density of foragers (ρ_f*) that minimizes total foraging time. The model predicts that colonies should

be selected to find ρ_f* because ρ_f is the only variable under immediate control of the colonies: ρ_s is set by the environment, F is constrained evolutionarily for each species, and E_s, D_s, and v_t are constrained by the physiology of the ants. However, ρ_f can be adjusted continually to minimize T_f based on changing seed densities.

By setting the derivative of T_f with respect to ρ_f equal to 0, we find ρ_f* which minimizes T_f: $-0.38 v_t^{-1} F^{1/2} \rho_f^{*-3/2} + \frac{1}{2} R E_s^{-1} D_s^{-1} (\rho_s - \frac{1}{2} R \rho_f^{*})^{-2} = 0$. Simplifying and solving for ρ_f^* gives $\rho_f^* = 0.76^{2/3} v_t^{-2/3} F^{1/3} E_s^{2/3} D_s^{2/3} R^{-2/3} (\rho_s - \frac{1}{2} R \rho_f)^{4/3}$ which can be simplified to:

$$\rho_f^* = 0.83 F^{1/3} T_s^{-4/3} (v_t R E_s D_s)^{-2/3} \qquad [4.8]$$

Table 4.1 ANTS variables, operational definitions and observed values[a]

Variable	Definition	Measurement Methods	Mean ±SE
Total population	Number of adult workers in a colony	Colony population was not measured in this study. Values are estimates from (1) Johnson 2000, (2) MacKay 2002, (3) Gordon 1984 and (4) Holldobler & Wilson 1990.	400[1,2] 500-2000[1,3] 10000[1,3,4]
T_f	Time of a foraging trip	Follow individual foragers from the time they leave the nest to the time they return with a seed. $T_f = T_t + T_s$.	712 ± 99 s 987 ± 131 s 846 ± 117 s
F	Number of foragers per colony	Measure the rate at which foragers leave (r_l) and enter (r_e) the nest by counting foragers for 3 minutes at 30 min. intervals. At equilibrium, $r_l = r_e$ and $F = r_l T_f$	110 ± 107 238 ± 142 1499 ± 127
d_t	Distance from nest to seed	Measure the linear distance between the seed and the nest.	4.8 ± 0.37 m 5.2 ± 0.49 m 8.2 ± 0.44 m
T_t	Roundtrip travel time from nest to search location	Follow foragers and record a) the time it takes to reach the search location and b) the time it takes from attaining a seed to returning to nest. The sum of these times is T_t.	275 ± 37 s 458 ± 49 s 456 ± 44 s
v_t	Travel velocity	$v_t = d_t/T_t$	0.037 ± 0.0032 m/s 0.029 ± 0.0039 m/s 0.042 ± 0.0038 m/s
T_s	Time spent searching for a seed	Measure the time interval between the start of search behavior to obtaining a seed.	436 ± 77 s 466 ± 102 s 356 ± 91 s
A	Territory area	Calculated as the area enclosed by a circle whose radius is twice the median seed distance	76.5± 28 m^2 72.1± 37 m^2 262.3± 33 m^2
ρ_f	Density of searching foragers in the territory of the colony	Averaged at the scale of the colony: $\rho_f = F/A$	0.43 ± 0.068 ants/m^2 0.84 ± 0.18 ants/m^2 1.58 ± 0.29 ants/m^2
		Averaged over 1m^2 quadrats within a territory: count the number of foragers searching within a 1m^2 quadrat in one instant (2004 only)	0.22±0.088 0.29±0.15 3.1±0.75
R	Number of foraging trips per ant per day	Time spent foraging per day divided by T_f	16± 1.8 11± 1.2 12± 1.5
ρ_s	Seed density	N/A	Unknown
Es	Search efficiency	N/A	Unknown
Ds	Search diffusion rate	N/A	Unknown

[a]Variables from the ANTS model with definitions, methods used to estimate each variable, and values observed for *P. desertorum, P. maricopa* and *P. rugosus*. All variables represent the mean for a species, averaged across multiple foragers and colonies of each species at the Sevilleta LTER and Portal, AZ.

Table 4.2 ANTS model predictions and observations

Description	Equation from Appendix 4.9		Observations
Prediction 1: Average distance of retrieved seeds (d_t) increases with the number of foragers (F) and decreases with the density of foragers (ρ_f).	$d_t = 0.38F^{1/2}\rho_f^{-1/2}$	[4.2]	Quantitatively consistent with prediction (Figure 4.3a)
Prediction 2: Average travel time (T_t) increases with F and decreases with ρ_f.	$T_t = 0.76\ F^{1/2}\rho_f^{-1/2}v_t^{-1}$	[4.3]	Quantitatively consistent with prediction (Figure 4.3b)
Prediction 3: The average search time of foragers (T_s) is inversely proportional to search efficiency (E_s), search diffusion rate (D_s) and seed density (ρ_s).	$T_s = (E_s D_s \rho_s)^{-1}$	[4.4]	Qualitatively consistent with the prediction that T_s decreases with ρ_s (Figure 4.5a) E_s and D_s were not measured.
Prediction 4: If E_s and D_s are constant, and ρ_s is not altered by external factors, then T_s increases throughout the foraging period as each forager removes a seed at rate R. T_s also increases ρ_f increases.	$T_s = [E_s D_s (\rho_s - \frac{1}{2} R\rho_f)]^{-1}$	[4.6]	Not consistent with prediction that T_s increases throughout foraging period (Section 4.6.3) Not consistent with prediction that T_s increases with ρ_f (Figure 4.5b)
Prediction 5: Optimal forager density (ρ_f^*) is the density of foragers that minimizes T_f. ρ_f^* increases with F.	$\rho_f^* = 0.83F^{1/3}\ T_s^{-4/3}\ (v_t R E_s D_s)^{-2/3}$	[4.8]	Qualitatively consistent with prediction that ρ_f^* increases with F (Figure 4.2c)
Prediction 6: T_f is found by substituting Equations 4.3 and 4.6 into Equation 4.1. If E_s, D_s, ρ_s, and v_t are equal across colony sizes, then T_f increases with F.	$T_f = 0.76F^{1/2}\rho_f^{-1/2}v_t^{-1} + [E_s D_s (\rho_s - \frac{1}{2} R\rho_f)]^{-1}$	[4.7]	Not consistent with prediction that T_f increases with F (Figure 4.2f)

Table 4.3 Comparison of ANTS variables between species and years [a]

	Between Species			Between Years	
Variable	*F* statistic	*p* value	Significant Differences	*F* statistic	*p* value
d_t	19.51	0.00012	*P. desertorum* < *P. maricopa* *P. desertorum* < *P. rugosus*	0.331	0.574
T_t	6.84	0.0094	*P. desertorum* < *P. maricopa* *P. desertorum* < *P. rugosus*	0.128	0.726
T_s	0.366	0.70	n.s.	1.89	0.19
T_f	1.44	0.27	n.s.	2.87	0.112
F	38.77	< 0.0001	*P. desertorum* < *P. rugosus* *P. maricopa* < *P. rugosus*	0.55	0.471
ρ_f	11.36	0.0014	*P. desertorum* < *P. rugosus*	0.757	0.399
A	11.03	0.0016	*P. desertorum* < *P. maricopa* *P. desertorum* < *P. rugosus* *P. maricopa* < *P. rugosus*	0.253	0.622

[a] Significant differences were determined using Tukey's method. The between species analysis includes both years. Removing the effect of year does not change which species are significantly different. The between years analysis includes all three species. The species-year interaction is only significant for T_s and T_f in *P. desertorum*.

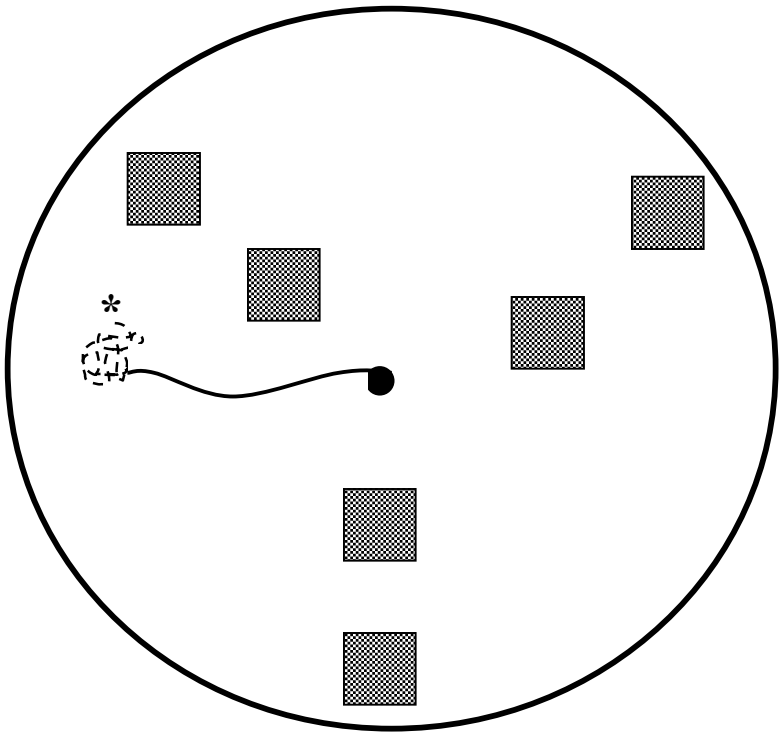

Figure 4.1 Method for measuring ANTS parameters in each colony. Foragers were followed as they left the nest entrance (black disk in the center). The outbound travel distance was measured as the length of the forager's relatively straight path from the nest entrance (solid line). The forager was followed as it searched (dashed line) until reaching a seed (asterisk). The seed distance was the linear distance from the seed to the nest entrance. 6 quadrats (shaded squares) were established in each colony in 2004. The quadrats were placed at two distances from the nest entrance and foraging activity was monitored inside the quadrats in 300 s intervals.

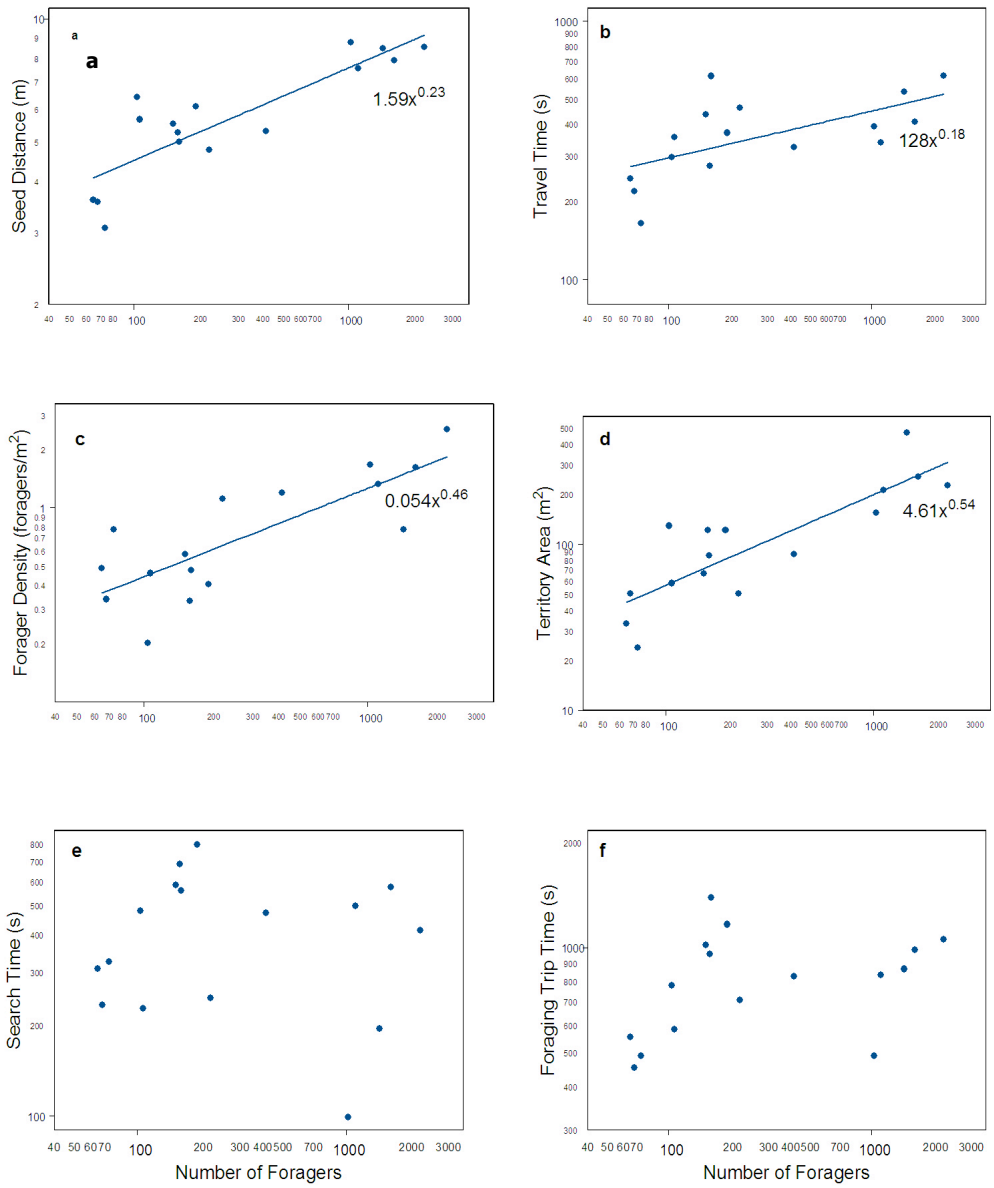

Figure 4.2 Observed colony properties as a function of forager population size. Each data point represents a colony. All axes are log transformed. **a**) Seed distance (p <0.001, r^2 = 0.74); **b**) travel time (p <0.011, r^2 = 0.38); **c**) forager density (p <0.001, r^2 = 0.64); **d**) area (p <0.001, r^2 = 0.72); **e**) search time (n.s., p = 0.726); **f**) foraging trip time (n.s., p = 0.185).

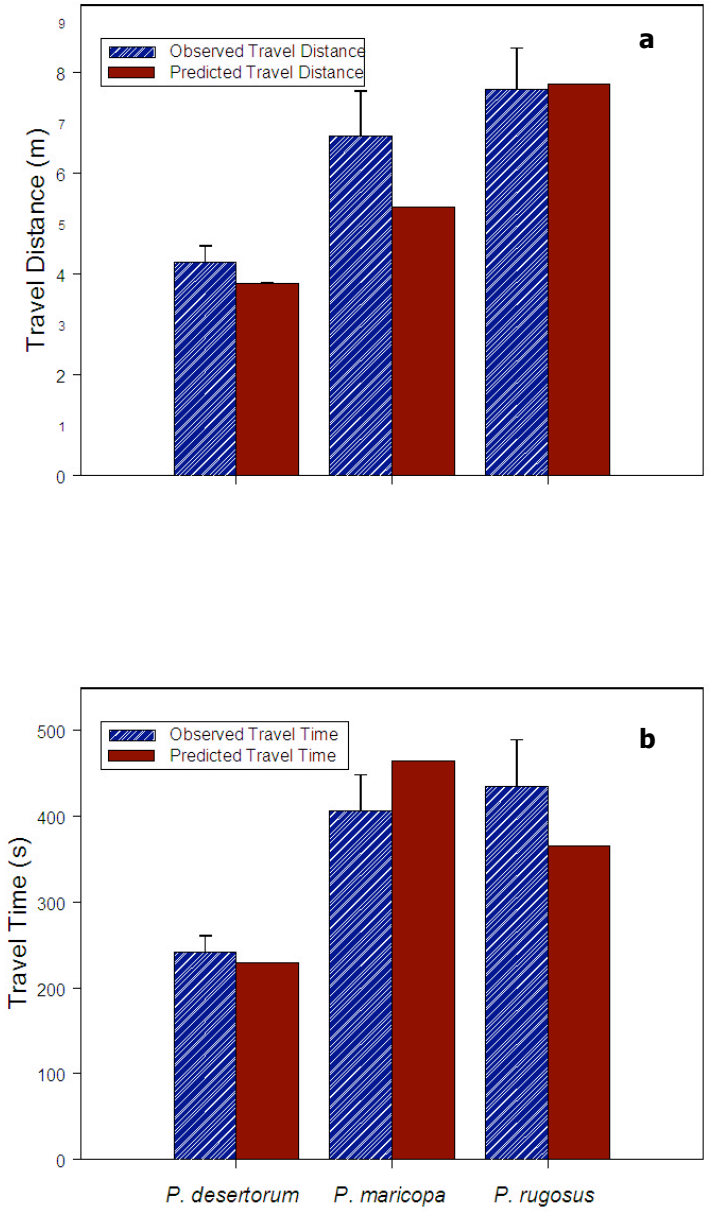

Figure 4.3 Predicted and observed travel times and distances. **a)** Travel distance predicted by ANTS Equation 4.2a and observed distance +SE. Travel distance predictions are indistinguishable from observations ($t = 0.445$, $p = 0.658$ for *P. desertorum*; $t = 0.0572$, $p = 0.955$ for *P. maricopa*; $t = -0.421$, $p = 0.676$ for *P. rugosus*). **b)** Travel time predicted by ANTS Equation 4.2b and observed travel time +SE. Travel time predictions are also indistinguishable from observations ($t = 0.704$, $p = 0.485$ for *P. desertorum*; $t = -1.612$, $p = 0.117$ for *P. maricopa*; $t = 1.257$, $p = 0.216$ for *P. rugosus*).

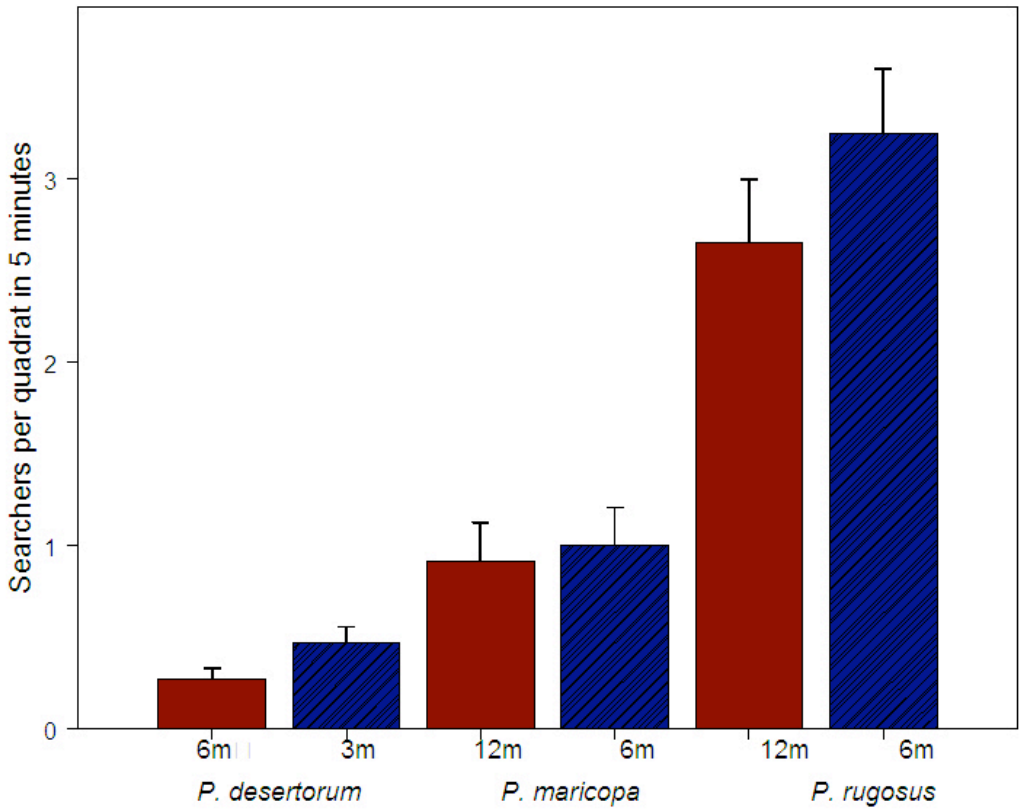

Figure 4.4 Mean number of foragers observed searching for seeds per quadrat under control conditions in 5 minute intervals + SE. The plots were located at the indicated distances from the nest entrances of each colony. The data shown is the mean for each colony of a given species.

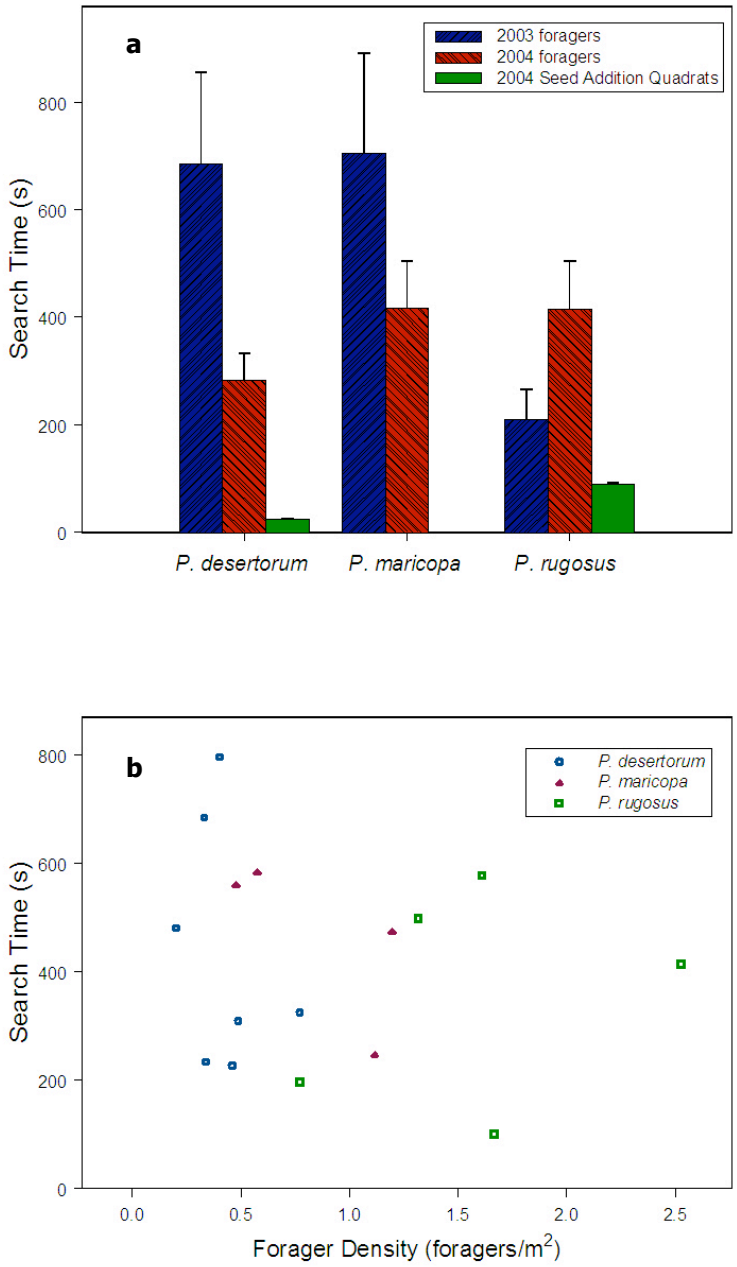

Figure 4.5 Search times in 2003 and 2004 **a)** Mean search time (+ SE) in 2003 and 2004 and in seed addition quadrats in 2004. **b)** Search time and forager density. Each point is a mean value for a colony. There is no significant relationship between T_s and ρ_f ($p = 0.485$).

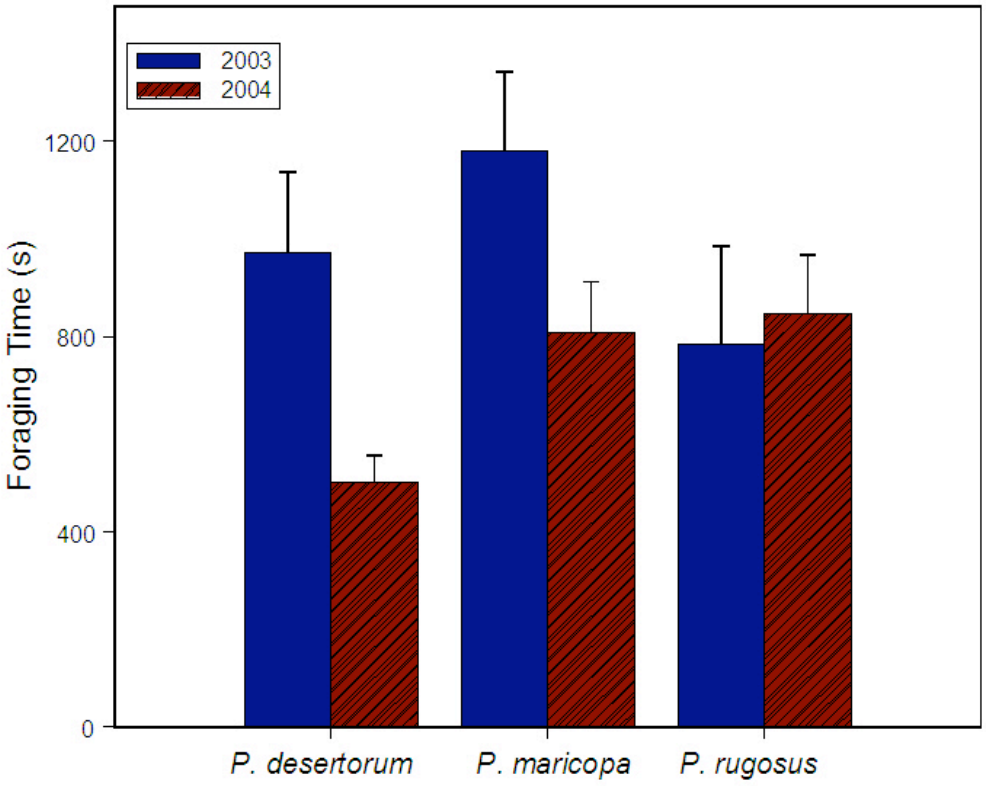

Figure 4.6 Mean (+SE) time of a foraging trip for each species in 2003 and 2004.

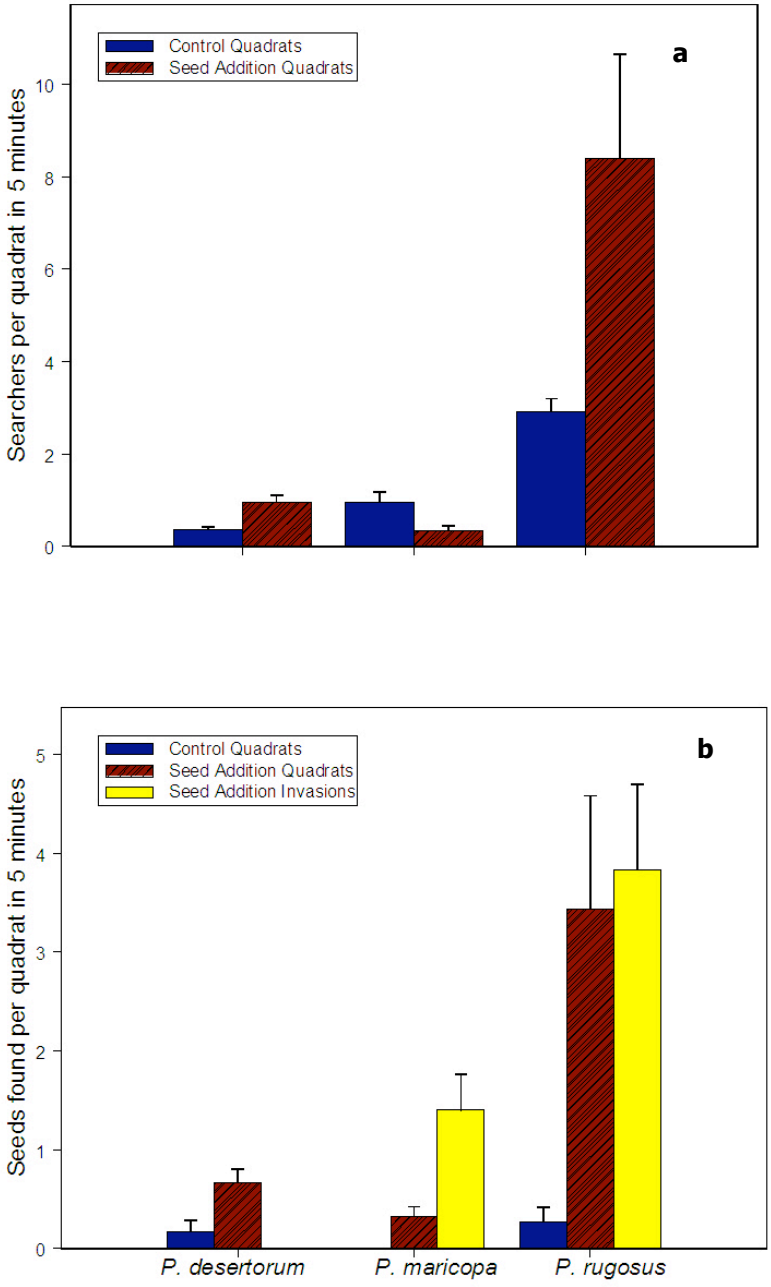

Figure 4.7 Number of searchers and seeds found in experimental quadrats. **a)** The mean (+SE) number of foragers searching in 1 m^2 quadrats in 300 s. Measurements were taken under natural conditions and during 2004 seed addition treatments for each species. **b**) Mean (+SE) number of seeds found in 300 s for each species in control quadrats, seed addition quadrats and quadrats of invaded territories.

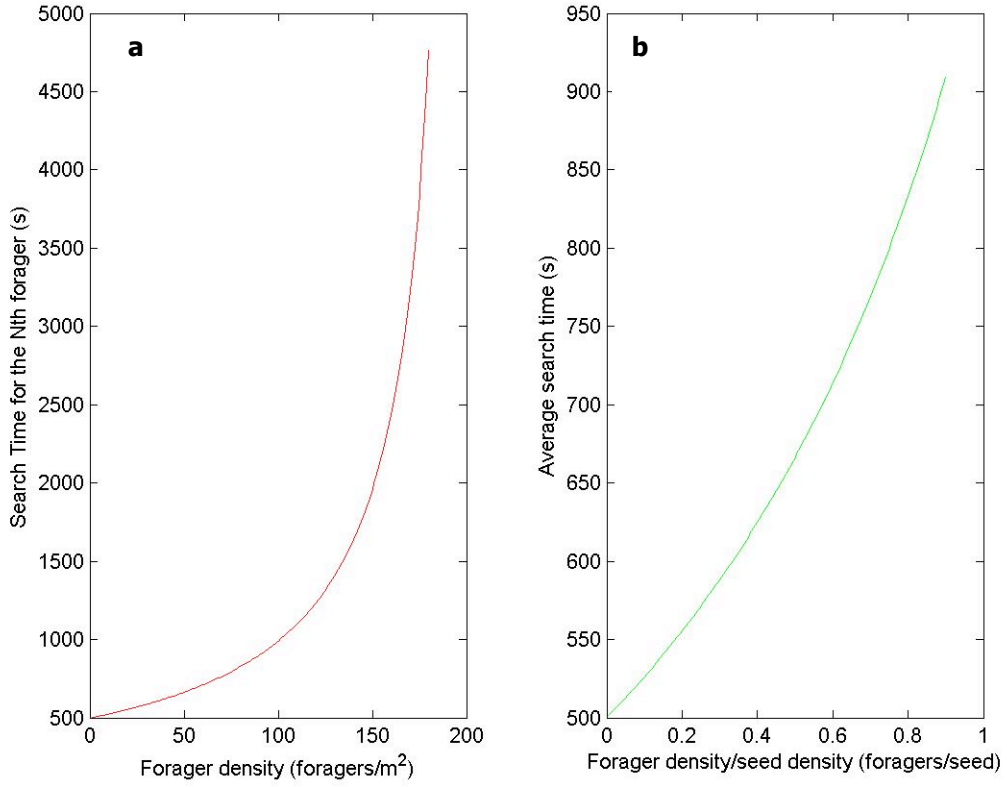

Figure 4.8 Predicted responses of search time to forager density and seed density. **a)** Search time of each individual forager as forager density is increased. **b)** Mean search time per forager (T_s), averaged over all foragers, as the density of foragers (ρ_f) approaches the density of seeds (ρ_s). $F = 2000$ and $\rho_s = 400$ in the simulations.

5 CONCLUSIONS: COMMON GEOMETRIC FOUNDATIONS OF METABOLIC SCALING IN INDIVIDUALS AND SOCIETIES

Just as individual organisms construct arteries and veins to distribute energy to cells throughout their bodies, societies construct distribution systems to transport energy and materials to individuals. In modern human societies, these distribution networks take the form of highways and airline routes, oil pipelines and electric grids, and numerous other physical and virtual systems that enable modern society to function. In ant colonies, social infrastructure includes foraging trails, pheromonal communication systems, and nest structure.

The hierarchical branching geometry of metabolic networks has been used to explain common scaling behaviors across levels of biological organization (West *et al.* 1999, Brown *et al.* 2004). Allometric scaling underlies the scaling of birth rate in individual mammals that is discussed in Chapter 3. It also appears to underlie metabolic processes in social organization that are discussed in Chapters 2 and 4, although there are important differences between metabolic networks in organisms and societies.

5.1 SCALING OF NETWORK SIZE IN INDIVIDUALS AND COLONIES

The 1/4 power scaling that is so pervasive in biological systems may have a more general cause than the specific geometry of fractal branching networks (Brown *et al.* in prep). In Chapter 4, I show that the distance each forager travels to acquire energy is dependent upon the size of its colony. I assume that the density of searching foragers (ρ_f) is constant

within a territory, that is, each forager searches an area of the same size, and all areas of the territory are searched. In section 4.9, I calculate the mean distance traveled by each forager (d_t) and the total distance traveled by all foragers ($d_{t\text{-}total}$) to search all areas of the territory. I assume that each forager takes the most direct path from the nest to the area it searches. $d_{t\text{-}total}$ is found by integrating the distances (d) that all foragers travel from the colony center to all search locations in the territory area: $d_{t\text{-}total} \sim \int_0^{d_{tmax}} \rho_f d^2 \, \delta d$. d_{tmax} is the maximum distance any forager travels and is proportional to $F^{1/2}\rho_f^{-1/2}$, where F is the number of foragers. $d_t \sim F^{1/2}\rho_f^{-1/2}$ and $d_{t\text{-}total} \sim F^{3/2}\rho_f^{-1/2}$. The length of the network can be pictured as filling a series of concentric hollow cylinders where the height of each cylinder is equal to the distance from the center.

If the ants foraged in primarily three-dimensional space (as might be the case for ants that forage in a volume of leaf litter), the network integrates the distances traveled by foragers searching the volume of the territory: $d_{t\text{-}total} \sim \int_0^{d_{tmax}} \rho_f d^3 \, \delta d$ where $d_{tmax} \sim F^{1/3}\rho_f^{-1/3}$. Solving this integral, $d_{t\text{-}total} \sim F^{4/3}\rho_f^{-1/3}$. More generally, for a given density of foragers, the size of the network increases faster than the number of foragers of which it is composed: $d_{t\text{-}total} \sim F^{(n+1)/n}\rho_f^{-1/n}$ where n is the dimension of the space searched by the foragers.

The same method may be used to describe the minimum size of a metabolic network in an organism. Instead of foragers leaving a central location to gather resources dispersed in the surrounding territory, imagine an individual with a central heart that must distribute blood to cells that fill the surrounding organism. Instead of each ant searching an invariant amount of space, imagine that each cell receives an invariant amount of

resource. In other words, imagine that the network is supplying resources at a rate proportional to the size of the organism.

In such a hypothetical organism, the distances traveled to fill the space of the organism are the same as in the distances traveled by a colony of ants foraging in three dimensions: $d_{t\text{-}total} \sim C^{4/3}\rho_c^{-1/3}$ where C is the number of cells to which resources travel and ρ_c is the density of cells (Brown *et al.* in prep). Since the density and mass of cells in organisms do not vary with respect to organism mass, then $C \sim M$ and $d_{t\text{-}total} \sim M^{4/3}$ where M is the mass of the organism. The hypothetical network delivers resources at rate B, such that $B \sim M$. Given $d_{t\text{-}total} \sim M^{4/3}$ and $B \sim M$, then $B \sim (d_{t\text{-}total})^{3/4}$. The metabolic output of the network is proportional to the network size raised to the 3/4 power.

In organisms, the size of the network does not grow faster than the organism itself. If that were the case, the network would take up an increasing percentage of the volume of larger organisms. Instead, the size of the network is directly proportional to body mass: $d_{t\text{-}total} \sim M^{1}$. For example, the volume of blood in mammals is proportional to body mass (Calder 1984, West *et al.* 1997). Since the output of a network is proportional to $(d_{t\text{-}total})^{3/4}$, the output of a network of size $d_{t\text{-}total} \sim M^{1}$ is proportional to $M^{3/4}$. Thus, in organisms, network size scales linearly with body mass, and metabolic rate scales with an exponent of 3/4. As a result, cellular metabolic rate scales as $M^{-1/4}$. As organisms and their metabolic demands increase, the cells that constitute the organism must slow down.

5.2 Scaling Differences Between Colonies and Individuals

Ant colonies have taken a different approach to accommodating the allometric scaling of network size. First, there is no physiological constraint that prevents the size of the foraging network from growing faster than the number of foragers who are searching. It is possible for an increasing percentage of F to be taken up by travelers. A large organism is not composed primarily of blood, but foragers in a large colony can spend most of their foraging time traveling rather than searching. This was observed in the *Pogonomyrmex*: foragers in large colonies had the longest travel times (Figure 4.3) and the shortest search times (Figure 4.5a).

Second, the density of ants varies with colony size. The largest *Pogonomyrmex* colonies had the highest density of foragers (Figure 4.2c). Since $d_{t\text{-}total} \sim F^{3/2}\rho_f^{-1/2}$, increasing density decreases network size. If density were constant, the ANTS model would predict $d_t \sim F^{1/2}$. However, in *Pogonomyrmex*, $\rho_f \sim F^{1/2}$ (Figure 4.2c), and as a result, $d_t \sim F^{1/4}$ (Figure 4.2.a). Thus, large colonies reduce travel distances and times by increasing forager density.

Increasing density in large colonies is analogous to diminishing cellular metabolic rate in a larger organism. Each ant has access to a smaller share of territory area, and if resource densities are constant, a smaller share of resources. Thus, in large colonies, the terminal branches of the network and the foragers are spaced more closely together, while in larger organisms, the cells are spaced at the same density regardless of body size, but the terminal branches of the metabolic network are spaced further apart. Both the amount

of resource to which the ant has access and the amount of resource delivered to the cells are lower in larger systems.

Foragers in a colony are different from cells in an organism because foragers have to spend time searching for their resources. In *Pogonomyrmex* the seed intake rate of the colony (B_{col}) is proportional to the number of foragers (F) divided by the average time of a foraging trip (T_f). If T_f were only composed of travel time (T_t), then we would expect $B_{col} \sim F/T_t$. Since $T_t \sim F^{1/4}$, then $B_{col} \sim F^{3/4}$, analogous to $B \sim M^{3/4}$ in organisms, even though the ants forage in two dimensions. However, allometric scaling of metabolic intake with colony size was not observed in *Pogonomyrmex* because foraging time is composed of search time in addition to travel time.

The need to search for food raises a third important way that foragers accommodate allometric scaling of network size. Ants in larger colonies appeared to utilize information to locate patches with high seed density and then extract more resources per unit area than small colonies (Figure 4.8). Even though foragers in large colonies had a higher density of foragers, each forager found seeds faster. Thus, large colonies compensate for increased density and increased travel time by foraging in high quality patches. This is contrary to the resource division patterns in mammals: larger mammals can persist on abundant, but lower quality, food patches (Brown *et al.* 1993, Ritchie & Olff 1999).

5.3 Extrapolating Metabolic Scaling to Human Societies

Space-filling metabolic networks integrate individual organisms and ant colonies by connecting all parts of the individual or the colony territory and enabling the organism or colony to function as a whole unit. The integration has mathematical consequences: integration introduces an additional dimension to distribution networks. Connecting all parts of a space via networks is a very general problem for which there are many solutions (Banavar *et al.* 1999, Fath *et al.* 2001, Gastner & Newman 2004a). The simplest network geometry, which integrates the shortest distances from a central location to all areas or volumes of a system, generates an allometric scaling of network delivery capacity with network size. Similar scaling may characterize the resource acquisition and distribution networks of human societies.

In individual organisms and ant colonies, metabolic materials travel between a central place and the volume of the organism or space of the territory. In human societies, material and energy are acquired from and delivered to dispersed locations. Resources are transported not only between central hubs and outlying locations, but also directly between distant locations. The networks in human societies are further complicated because the dimensions of the space they fill are unclear. While roads and railways appear to function in two dimensions, other networks such as airline routes and the Internet may function at much higher dimensionality (Gastner & Newman 2004b). Additionally, as seen in the *Pogonomyrmex*, extending networks beyond organisms and exploiting information about the environment can change the scaling relationship between the size of a system and its metabolic rate.

Despite such complications, the way that network scaling affects foraging in colonies may shed light on how metabolic consumption influences human societies. For example, the work a colony must do to acquire seeds increases faster than the number of foragers. That is analogous to diminishing returns to complexity in human societies (Tainter 1990). As societies grow and become more complex, more and more work goes into sustaining the society (acquiring, transporting and defending resources) rather than directly delivering services and resources to the population.

Agricultural production in the twentieth century provides an illustrative case of diminishing returns. Agricultural yield increased 6-fold, but the industrial metabolism which produced that yield increased 150-fold (Smil 2000). Diminishing returns are also evident in the Ontogenetic Growth Model (West *et al.* 2001). As an organism approaches its maximum size, more and more of its metabolism is allocated to maintenance, and less is available for growth and reproduction.

Hall *et al.* (1986) define the energy return on investment (EROI) as energy acquired divided by the energy spent to acquire it. Tainter *et al.* (2003) suggest that large organisms and consumptive societies must either utilize high quality resources or increase social organization to acquire sufficient low quality resources. Metabolic theory provides a quantitative framework for measuring how the size of a social system affects the cost of building infrastructure to acquire and distribute resources.

While humans appear to have evolved the same reproductive allocation strategies as other mammals, modern humans also exist in a social context. Human societies have evolved networks at a higher level of organization. The rate at which those networks deliver resources appears to constrain human ecology and life history.

5.4 REFERENCES

Banavar, J.R., Maritan, A. & Rinaldo, A. (1999). Size and form in efficient transportation networks. *Nature*, **399**, 130–132.

Brown, J.H., Gillooly, J.F., Allen, A.P., Savage, V.M. & West, G.B. (2004). Toward a metabolic theory of ecology. *Ecology,* **85**, 1771-1789.

Brown, J.H., Marquet, P.A. & Taper, M.L. (1993). Evolution of body size: Consequences of an energetic definition of fitness. *Am. Nat.,* **142**, 574-584.

Brown, J.H., Sibly, R.M., Gillooly, J.F., & West, G.B (in preparation). A general geometric explanation for quarter power scaling in biology.

Calder, W.A. (1984). *Size, Function and Life History*. Harvard Univ. Press, Cambridge, MA.

Fath, B.D., Patten, B.C., & Choi, J.S. (2001). Complementarity of ecological goal functions. *J. Theor. Biol.*, **208**, 493-506.

Gastner, M.T. & Newman, M.E.J. (2004a).The spatial structure of networks. *arXiv:cond-mat*/0407680.

Gastner, M.T. & Newman, M.E.J. (2004b). Shape and efficiency in spatial distribution networks. *arXiv:cond-mat*/0409702.

Hall, C.A.S., Cleveland, C.J., & Kaufmann, R. (1986). *Energy and resource quality*. Wiley, New York.

Ritchie, M.E., & Olff, H. (1999). Spatial scaling laws yield a synthetic theory of diversity. *Nature,* **400**, 557–560.

Smil, V. (2000). Energy in the twentieth century: Resources, conversions, costs, uses, and consequences. *Annu. Rev. Energy Environ*., **25**, 21-51.

Tainter, J. (1990). *The Collapse of Complex Societies*. Cambridge University Press, Cambridge.

Tainter, J. A., T. F. H. Allen, Little, A. & Hoekstra, T.W. (2003). Resource transitions and energy gain: Contexts of organization. *Cons. Ecol*., **7**, 4.

West, G.B., Brown, J.H., & Enquist, B.J. (1997). A general model for the origin of allometric scaling laws in biology. *Science,* **276**, 122–126.

West, G.B., Brown, J.H. & Enquist, B.J. (1999). The fourth dimension of life: Fractal geometry and allometric scaling of organisms. *Science,* **284**, 1677–1679.

West, G.B, Brown, J.H. & Enquist, B.J. (2001). A general model for ontogenetic growth. *Nature,* **413,** 628-631.